The FEBS Journal

FEBS PRESS science publishing by scientists

Extracellular matrix composition modulates PDAC parenchymal and stem cell plasticity and behavior through the secretome

Giulia Biondani[1,†,‡,§], Katrine Zeeberg[2,§], Maria Raffaella Greco[2,§], Stefania Cannone[2], Ilaria Dando[1], Elisa Dalla Pozza[1], Maria Mastrodonato[3], Stefania Forciniti[1], Valeria Casavola[2], Marta Palmieri[1], Stephan Joel Reshkin[2] and Rosa Angela Cardone[2]

1 Department of Neuroscience, Biomedicine and Movement, Biochemistry Section, University of Verona, Italy
2 Department of Biosciences, Biotechnology and Biopharmaceutics, University of Bari, Italy
3 Department of Biology, University of Bari, Italy

Keywords
3D organotypic cultures; cancer stem cells; desmoplastic reaction; pancreatic adenocarcinoma; vasculogenic mimicry; VEFGR-2

Correspondence
S. J. Reshkin and R. A. Cardone, Department of Biosciences, Biotechnology and Biopharmaceutics, Via E. Orabona, 4, 70126 Bari, Italy
Fax: +39 080 5443388
Tel: +39 080 5443385
E-mails: stephanjoel.reshkin@uniba.it; rosaangela.cardone@uniba.it
and
M. Palmieri, Department of Neuroscience, Biomedicine and Movement, Biochemistry Section, Strada Le Grazie, 8, 37134 Verona, Italy
Fax: +39 045 802 7170
Tel: +39 045 802 7169
E-mail: marta.palmieri@univr.it

[†]**Present address**
INSERM U1065, Team 4 Leukemia: Molecular addictions, Resistances & Leukemic Stem Cells, Mediterranean Centre for Molecular Medicine (C3M), Nice, France

[‡]**Present address**
Faculté de Médecine, Université di Nice, Sophia Antipolis, Nice, France

[§]These authors contributed equally.

(Received 14 September 2017, revised 5 March 2018, accepted 6 April 2018)

doi:10.1111/febs.14471

Pancreatic ductal adenocarcinoma (PDAC) is one of the most lethal cancers. Its aggressiveness is driven by an intense fibrotic desmoplastic reaction in which the increasingly collagen I-rich extracellular matrix (ECM) and several cell types, including cancer stem cells (CSCs), create a tumor-supportive environment. However, how ECM composition regulates CSC dynamics and their relationship with the principle parenchymal tumor population to promote early invasive growth is not yet characterized. For this, we utilized a platform of 3D organotypic cultures composed of laminin-rich Matrigel, representative of an early tumor, plus increasing concentrations of collagen I to simulate malignant stroma progression. As ECM collagen I increases, CSCs progress from a rapidly growing, vascular phenotype to a slower growing, avascular phase, while maintaining their endothelial-like gene signatures. This transition is supported autocrinically by the CSCs and paracrinically by the parenchymal cells via their ECM-dependent secretomes. Indeed, when growing on an early tumor ECM, the CSCs are dedicated toward the preparation of a vascular niche by (a) activating their growth program, (b) secreting high levels of proangiogenic factors which stimulate both angiogenesis and vasculogenic mimicry, and (c) overexpressing VEGFR-2, which is activated by VEGF secreted by both the CSC and parenchymal cells. On Matrigel, the more differentiated parenchymal tumor cell population had reduced growth but a high invasive capacity. This concerted high local invasion of parenchymal cells into the CSC-derived vascular network suggests that a symbiotic relationship between the parenchymal cells and the CSCs underlies the initiation and maintenance of early PDAC infiltration and metastasis.

Abbreviations
2D, two-dimensional culture; 3D, three-dimensional culture; C, collagen I; CCM, collagen I-derived conditioned medium; CM, conditioned medium; CSC, cancer stem cells; ECM, extracellular matrix; M, Matrigel; MCM, Matrigel-derived conditioned medium; PDAC, pancreatic adenocarcinoma; VEGF, vascular endothelial growth factor; VEGFR-2, vascular endothelial growth factor receptor 2; VM, vasculogenic mimicry.

Introduction

Pancreatic ductal adenocarcinoma (PDAC), the most frequent type of cancer of the pancreas (90% of all cases) [1], is a deadly disease with a 5-year survival rate of approximately 5% [2]. There has been very little improvement in the clinical outcome for this devastating disease during the past 30 years [3] and it is projected to become the second cause of cancer-related deaths in the next 10–15 years [4].

One of the hallmarks making PDAC so aggressive is the bidirectional interaction between the cancer cells and their prominent, surrounding stromal microenvironment (desmoplasia), which can account up to 90% of PDAC tissue [5]. Desmoplasia is a tumor-supportive, highly reactive environment consisting of the cancer and accessory cells (including cancer-associated fibroblasts, endothelial, and immune cells) embedded in a dense stroma of extracellular matrix (ECM) components (fibronectin, proteoglycans, hyaluronic acid, growth factors, proteinases, and ever more collagen type I as the tumor progresses) [6], [7]. This is particularly true for PDAC where collagen I can constitute up to 80% of the tumor space and is associated with a worsened outcome [8,9]. The collagen I-rich stromal environment extrinsically stimulates maligant cell properties (i.e., proliferation, invasion, survival, and immune tolerance), which are already intrinsically hyperactivated in PDAC, thus promoting tumor growth, early invasion and chemo-radiation resistance [10]. In addition, desmoplasia represents a niche for the development of a small subset of the cancer cell population, cancer stem cells (CSCs) [11], which retain cancer-initiating potential, self-renewal, and multilineage differentiation capabilities (stemness). This contributes to the tumor heterogeneity, including the ability to express an endothelial-like phenotype and participate in tumor neovascularization via the formation of a blood-conducting, matrix-rich meshwork, known as "vasculogenic mimicry" (VM), all of which critically influences tumorigenesis, metastasis, and drug resistance [12]. CSCs have been demonstrated in PDAC [13–18] and have been shown to be a highly dynamic tumor subpopulation [14,19].

It is now widely recognized that the various cellular components in the microenvironment influence and can even dominate genotypic changes in malignant cells [20,21] and cancer stem cells [22]. Furthermore, the ECM plays a fundamental role in directing normal cell development [23] and normal stem cell fate/plasticity [24]. However, relatively little is known about the specific role of the ECM composition of the tumor desmoplastic microenvironment and its interaction with the different tumor cell populations (parenchymal and CSCs) in determining their growth, phenotypic plasticity, reciprocal cross talk, and in driving tumor progression.

It is, therefore, critical to establish more physiologically relevant *in vitro* experimental models allowing the study of PDAC biology, therapeutic targets, and drug efficacy in the context of the "desmoplastic tumor-supportive" environment. In this regard, three-dimensional (3D) cultures are a relevant preclinical model with advantages over 2D monolayers as they more accurately reflect the architecture and biomechanical properties of the tumor [25–27]. This led us to use 3D systems in our experiments to mimic and study the influence of the ECM microenvironment on PDAC cells, settling on organotypic cultures on combinations of ECM components with increasing collagen I concentrations in order to model PDAC progression [28]. The organotypic model offers many advantages over other 3D protocols including the ability to easily manipulate the ECM to mimic the different stages of PDAC progression and to produce complex coculture conditions [27].

Here, utilizing these organotypic cultures, we find that the different compositions of the tumor ECM actively affected, via ECM–cell interactions, the growth kinetics, morphology, invasion, and the secretome profiles of a highly aggressive PDAC parenchymal cell line, Panc1 [29], and their derived CSCs. Furthermore, we demonstrate that the ECM composition also plays a critical role in the generation of a complex and highly dynamic cross talk between the two cell lines which, via the secretion of VEGF and other proangiogenic/growth factors, reciprocally influences their same growth dynamics and phenotypic plasticity. Altogether, these findings propose a scenario in which the ECM composition and the cellular secretome cooperate to jointly regulate both growth and morphology of the Parental and CSC cell lines and, by modulating the highly dynamic interactions between them, establishes a continuum between tumor initiation and progression in primary PDAC tumors.

Results

We have previously reported that in 2D culture, CSCs derived from the PDAC cell line, Panc1, exhibited an increase in the stem cell markers EpCAM and CD44v6 and acquisition of a mesenchymal phenotype, in comparison to their Parental counterpart [14]. Furthermore, in line with the reported low-proliferative ability of CSCs [30,31], they grew significantly slower than Parental cells in 2D culture [14]. Altogether these

results confirmed that CSCs isolated from the Parental Panc1 cell line and cultured in 2D in their selection medium possess stemness features, both phenotypically and genotypically.

As cell growth dynamics are quite different when assessed in 3D [32], and PDAC is characterized by a dense fibrotic desmoplastic reaction highly affecting pancreatic cancer growth [33], we developed 3D organotypic models based on different matrix compositions to simulate the *in vivo* tumor stroma associated with PDAC progression. For this, CSCs or Parental cells were seeded on the organotypic setup consisting of 100% Matrigel (a laminin-rich ECM biomimetic of an early-stage tumor), or a mix of 90% Matrigel:10% collagen I (90M/10C), 70% Matrigel:30% collagen I (70M/30C), 20% Matrigel:80% collagen I (20M/80C), and finally on 100% collagen I, since collagen I is increasingly enriched in the ECM as PDAC develops [34].

In CSCs, stem cell marker expression is sensitive to ECM composition

We first determined the effect of matrix composition on the expression of the typical stem cell surface marker, CD44v6, and on the adhesion molecule, E-cadherin [14], when the two cell lines grow on ECMs at increasing collagen I content. Importantly, we found that mRNA levels of CD44v6 were strictly dependent on the ECM composition in CSCs. Indeed, CD44v6 expression was maximum on Matrigel (two-fold compared to their 2D growth) and was reduced stepwise as collagen I increased in the ECM (Fig. 1A). On the other hand, the mRNA levels of E-cadherin decreased in 3D (vs 2D) only in the CSCs and this reduction was also ECM-dependent, in that E-cadherin levels were minimum for cells grown on 100% Matrigel and increased stepwise as collagen I increased in the ECM (Fig. 1D). Importantly, it has been demonstrated that E-cadherin expression inversely correlates to the CSC number, *in vitro* cell proliferation/migration, and *in vivo* tumor vascularization [35].

Parental and CSC phenotype, growth rate, and invasion are dependent on ECM composition

We then went on to determine the effect of ECM composition on growth morphology and rate and on invasive capacity and mechanism. Importantly, not only were the CSCs able to attach to all the ECMs but

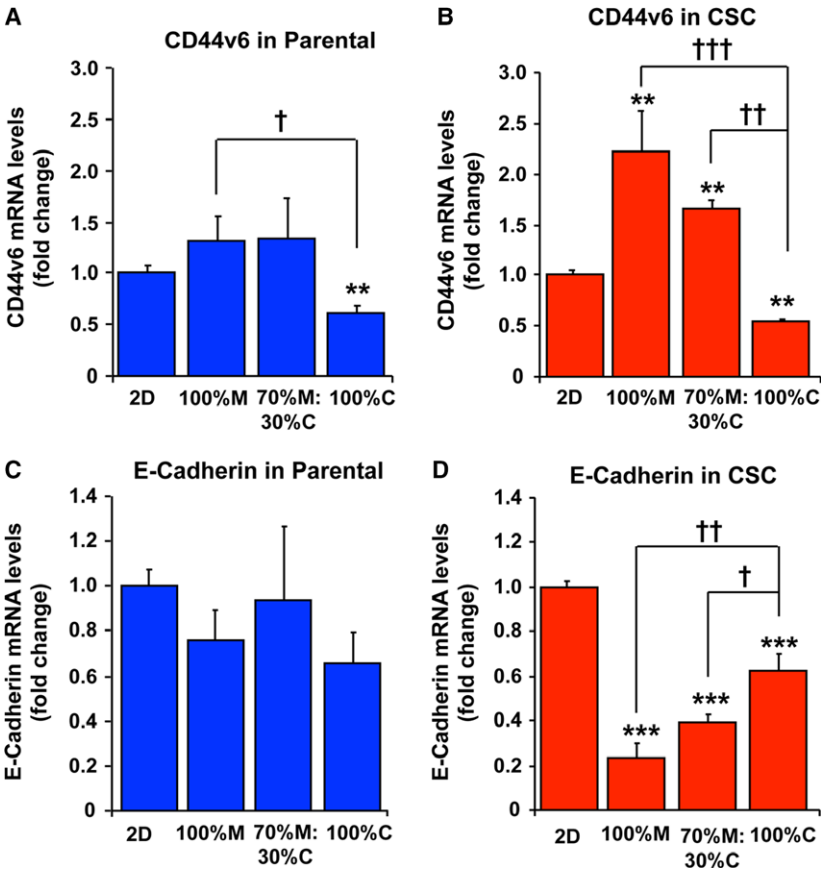

Fig. 1. ECM composition affects Parental and CSC expression of CD44v6 and E-cadherin. Histograms of CD44v6 (A and B) and E-Cadherin (C and D) mRNA levels in Parental cell and CSC that had been cultured on 100% Matrigel, 70% Matrigel:30% collagen I, or 100% collagen I as described in Materials and methods. Real-time PCR values are the means (± SEM) of three independent experiments each performed in triplicate and are reported as fold change relative to levels in 2D culture $^{*}P < 0.05$, $^{**}P < 0.01$, $^{***}P < 0.001$, or relative to different ECM compositions $^{\dagger}P < 0.05$, $^{\dagger\dagger}P < 0.001$, and $^{\dagger\dagger\dagger}P < 0.001$.

both cell lines also changed their growth morphological phenotypes and invasive ability depending on the ECM composition (Fig. 2A). Particularly interesting was the distinct morphologies of the two cell lines when grown on 100% Matrigel. Indeed, the Parental cells grew as small discrete, clonal colonies deriving from single cells, while the CSCs formed a structured vascular-like, network lining lacunae and resembling VM [30]. As the amount of collagen I increased, both the CSC and Parental cell lines lost their highly organized growth morphologies and grew instead more as monolayers with only small differences between them (Fig. 2A), suggesting that the ECM composition has a crucial role on cell plasticity and the acquisition of the final morphology.

In particular, the vascular-like structures formed by the CSCs on 100% Matrigel were reduced as collagen I levels increased (21.4 ± 3.1 vs 8 ± 2.3 lacunae/field in 100% Matrigel vs 70%Matrigel/30% collagen I, respectively, $P < 0.001$) and completely disrupted as collagen I levels surpassed 30% of the ECM composition. This loss of VM organization with higher collagen I content corresponds well with increased collagen I representing the late-state PDAC. Indeed, VM formation is reported to be mainly found in early-state cancers and is decreased during tumor progression [36], further supporting the above morphological data and the use of the organotypic culture systems as representative of PDAC progression.

To assess whether the ECM composition would also affect the kinetics of cell growth, CSCs and Parental cells were seeded on either 100% Matrigel, 70% Matrigel:30% collagen I, or 100% collagen I and growth at day 0, 3, and 7 was monitored as described in Methods (Fig. 2B). When grown on 100% Matrigel, the CSCs exhibited a significantly higher growth rate (doubling time in days (Td) = 1.77 ± 0.17) that was reduced as collagen I increased (from Td = 2.77 ± 0.25 to Td = 7.48 ± 3.1 cultured on 30% and 100% collagen I, respectively). The Parental cells had a similar pattern but grew much more slowly on all ECM compositions than the CSCs (Td = 3.75 ± 0.48 vs Td = 4.45 ± 0.34 vs Td=7.68 ± 2.13 cultured on 100% Matrigel, and 30% and 100% collagen I, respectively). The increased growth rate of CSCs compared to Parental cells on Matrigel (CSCs 2.11 ± 0.18-fold faster than Parental cells) corresponds to an inversion of their growth rates when measured in 2D conditions [14].

We then analyzed the role of the ECM composition in regulating the invasive phenotype of the Parental cells and CSCs, by measuring both their invadopodia-mediated ECM proteolytic activity defined by their Digestion Index [37] (Fig. 2C,D) and their invasion (Fig. 2E) when the two cell lines grew on an early-stage tumor ECM (100% Matrigel) or a high-grade tumor ECM (20%Matrigel: 80% collagen I, 20M/80C). Interestingly, we found that Parental cells had a greatly increased ability to form functional invadopodia and digest the two types of ECM compared to CSCs, with a net higher Digestion Index when cultured on 100%M with respect to 80%C/20%M. This higher level of ECM-degrading activity for Parental cells compared to CSCs correlated with an increased Parental cell ability to invade across the two ECMs coating porous filters in Boyden Chamber chemoinvasion assays (Fig. 2E).

CSCs in nude mice develop proliferating and hypervascular tumors

In Figures 2A,B, CSCs and Parental cells respond to the different ECM compositions by changing both their growth pattern and growth rate kinetics. To determine if these *in vitro* behaviors of cells growing on Matrigel were retained *in vivo*, we produced early stage, confined tumors by subcutaneously injecting Parental cells or CSCs into nude mice.

We first evaluated whether the CSC's ability to organize into vessel-like networks when grown on Matrigel was reflected by an increased ability to promote a vascular network in the *in vivo* tumors. Histological assessment of the vascular network was performed on the tumor sections using Masson's trichrome stain, which highlights connective tissue and vascular thin walls. Excluding peripheral murine vessels and counting only vessels with a clearly identifiable lumen often containing red blood cells (RBCs), tumors originating from CSCs had a significantly higher number of vessels compared to tumors originating from Parental cells (4.7 ± 0.25 vs 3.4 ± 0.34 identifiable vessels *per* field (± SEM) of CSC vs Parental cell produced tumors, respectively, $n = 5$, $P = 0.002$). Furthermore, vessels in CSC-derived tumors were larger and had much more RBCs compared to those formed by Parental cells (Fig. 2F left panels). Interestingly, the low level of vascularization in Parental-derived tumors was associated with the presence of extended collagen-rich fibrotic regions (showed in blue), indicative of a higher level of fibrosis [38].

We then determined if the above-reported inversion of CSC and Parental cell *in vitro* growth rate on 3D (Matrigel) compared to 2D (Fig. 2B), which is in line with the reported observation that subcutaneous CSC-derived PDAC tumors grew 2.48 ± 0.34-fold larger than Parental cell-derived tumors [14], was due to an increased proliferative ability of CSCs compared to Parental cells. For this, the expression of the proliferation

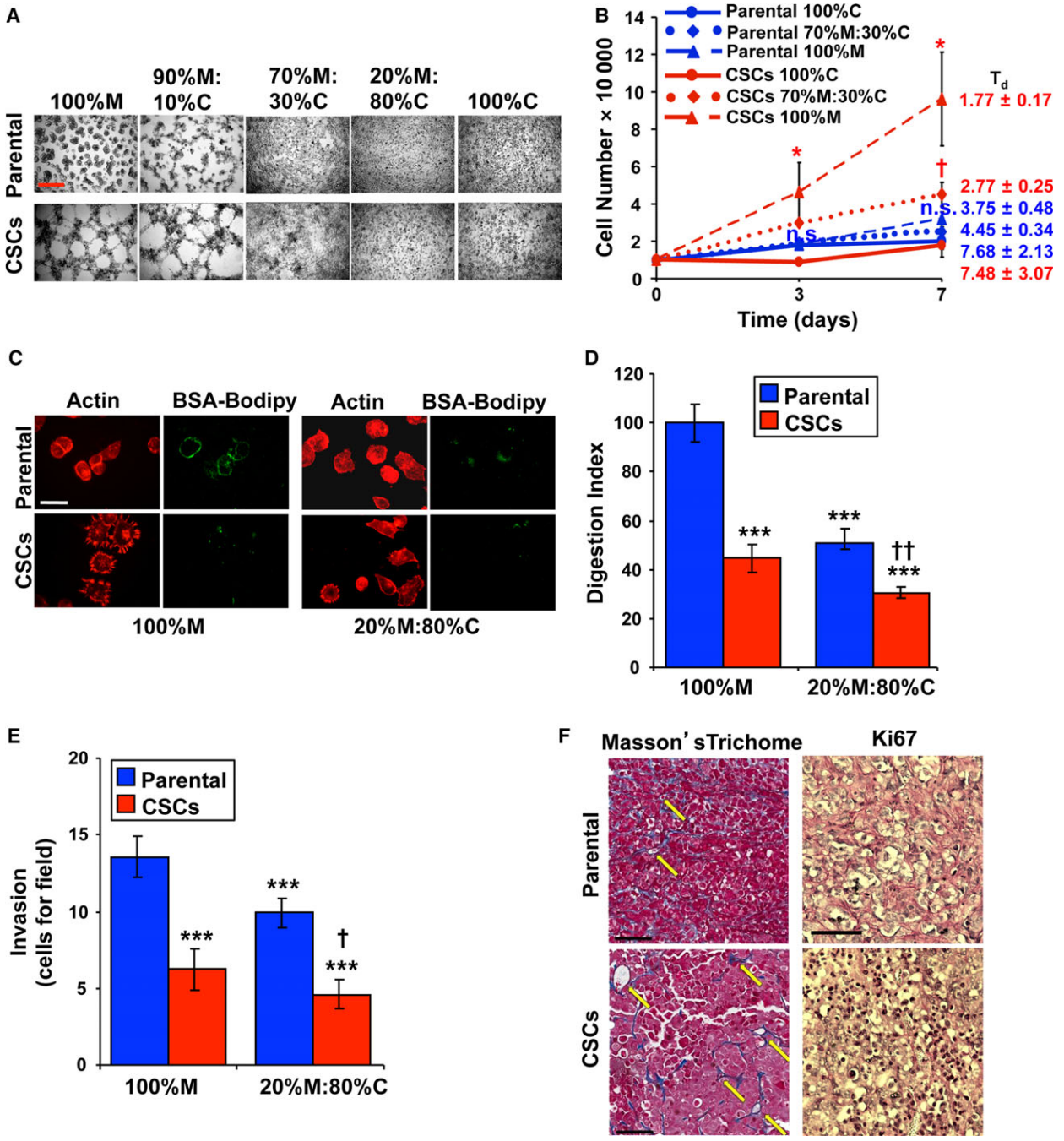

marker, Ki67, was analyzed by IHC in the subcutaneous tumor sections. Figure 2F (right panels) shows that, in line with the increased CSC growth rate on Matrigel and CSC-derived tumor size, the tumors formed by the CSC population also had a greatly increased proliferation compared to the tumor formed from the Parental cell population (194.3 ± 46.8 vs 60.2 ± 14 Ki67-positive nuclei/field CSC vs Parental, $n = 5$, $P < 0.001$).

Altogether, these *in vivo* results confirmed that the organotypic setting mimicking the initial stages of tumor development (low collagen I ECM), indeed, successfully predicted the increased ability of CSCs to induce a hyper-proliferative, blood-conductive vascular network in the primary tumor, growing ectopically (without signs of local infiltration and/or distant metastases) in an early-stage xenograft tumor model [39].

Fig. 2. ECM composition affects Parental and CSC growth, phenotype, and angiogenic capacity. A) Representative microscopic images of growth characteristics and phenotypic changes of Panc1-Parental cell line and their derived CSCs cultured on organotypic cultures composed of 100% Matrigel, 90% Matrigel:10% collagen I, 70% Matrigel:30% collagen I, 20% Matrigel:80% collagen I, and 100% collagen I. Scale bar represents 500 μm for all images. (B) Parental cell and CSC growth rates in organotypic cultures of 100% Matrigel, 70% Matrigel:30% collagen I, and 100% collagen I. Growth curves of Parental cells and CSCs cultured on the different ECMs were calculated from Resazurin reduction assays according to the standard curves obtained by fluorescence readings of Resazurin as described in Materials and methods. Growth assays were performed on day 0 (6 h after cell seeding), day 3, and day 7. Parental and CSC doubling times (Td) were calculated from each growth curve as described in Materials and methods. Data are mean ± SEM, $n = 5$, $^{*}P < 0.05$. (C & D) Invadopodia proteolytic activity of Parental cells and CSCs on 100% Matrigel or 20%Matrigel/80% collagen I as described in Materials and methods. (C) Typical images of actin expression and focal digestion of ECM mixed with BSA-Bodipy which produces green fluorescence within a black background. Scale bar, 50 μm. (D) Quantification of ECM degradation was performed as described in Materials and methods. ECM degradation was analyzed as total focal digestive activity of 100 cells (Digestion Index) and standardized to 100% for Parental cell activity. Data are mean ± SEM, $n = 5$, $^{***}P < 0.001$ compared to Parental cell activity on 100% Matrigel; $^{\dagger\dagger}P < 0.01$ compared to Parental cell activity on 80%C/20%M. (E) Invasive capacity of Parental cells and CSCs across ECM-coated filters in Boyden chambers in three independent experiments conducted in triplicate. Data are mean ± SEM, $^{***}P < 0.001$ compared to Parental cell invasion on 100% Matrigel; $^{\dagger}P < 0.05$ compared to Parental cell invasion on 80%C/20%M. (F) Masson's trichrome stain and immunostaining for Ki67. Parental cells or CSCs (1×10^5 cells/mouse) were subcutaneously injected into nude female mice. Tumors were extracted, fixed, and sectioned as in Materials and methods. Left panels: Masson's trichrome stain of representative tumor tissues derived from Parental cells and CSCs (scale bar, 100 μm). Vessels are lined with blue staining and possess hole lumens (yellow arrows). CSCs developed a vascular network with large caliber vessels in nude mice. Right panels: expression of Ki67 in these tumor samples was detected by IHC and then counterstained for hematoxylin. Scale bar, 100 μm.

CSCs have an increased expression of endothelial cell markers that are associated *in vivo* with vasculogenic mimicry

To determine whether the CSC vascular-like morphology acquired when grown on Matrigel and its stepwise loss with increasing collagen I content was associated with the basal expression of an endothelial-like phenotype, we analyzed mRNA expression levels of the endothelial cell markers CD34 and CD31 and the endothelium-associated marker CD144. The Parental cell line and CSCs were grown in 2D and in 3D on either 100% Matrigel, 70%M/30%C, or 100% collagen I. After 5 days, cells were collected and RNA was extracted, reverse transcribed, and analyzed by qPCR. When grown in 2D, the CSCs had a significantly higher expression of all three markers with respect to the Parental cells (26.6 ± 3.5, 6.4 ± 0.6, and 4.5 ± 0.1-fold for CD34, CD31, and CD144, respectively), suggesting that the CSCs intrinsically express higher levels of endothelial genes. When the cells were cultured in 3D (Fig. 3A-C), the mRNA expression levels of all three markers remained higher in the CSCs (red bars) compared to Parental cells (blue bars). We then evaluated whether this increased expression of CD31 and CD34 was associated with the CSC's increased ability to promote a vascular network *in vivo* compared to the tumor formed by Parental cells (Fig. 2F). Sections from the CSC- or Parental cell-derived subcutaneous tumors were immunostained for either human CD31 or human CD34 and counterstained for periodic acid–Schiff (PAS), a marker of VM [40]. Figures 3D demonstrate that almost all the vessels in the CSC-derived tumors displayed both CD31/CD34 and PAS staining while very few vessels in the Parental tumors were both PAS+ and CD31 + / CD34 + (4.3 ± 0.33 vs 1.7 ± 0.91 double-stained vessels *per* field (mean ± SEM), respectively, $n = 20$, $P < 0.0001$). Furthermore, the vessels in the CSC-derived tumor were larger, more complex and contained more erythrocytes. Altogether, these data indicate that the CSCs express the endothelial gene repertoire both in 2D and in all 3D conditions but that the full expression of the vascular (VM) phenotype is dependent on the ECM composition and could involve the secretion of proangiogenic factors.

Angiogenic and Growth Factor secretomes of Parental cells and CSCs are differently regulated by the ECM composition

As the vascular-like phenotype could be strongly influenced by the balance of pro- and antiangiogenic cellular factors secreted into the cell culture medium (secretome), we investigated if and how the different ECM compositions could modulate the above-observed different CSC and Parental growth phenotypes through changes in their angiogenic secretome by using an antibody array, where the protein expression level for each secreted factor was normalized to the positive internal controls (Fig. 4A,B). We started by using the array to profile the CSC's angiogenic secretome when cells grew for 6 days on 100% Matrigel as vessel-like structures, on 100% collagen I as monolayers, or on mixtures thereof (80M/20C and 70M/30C). We found that the secreted factors fell into

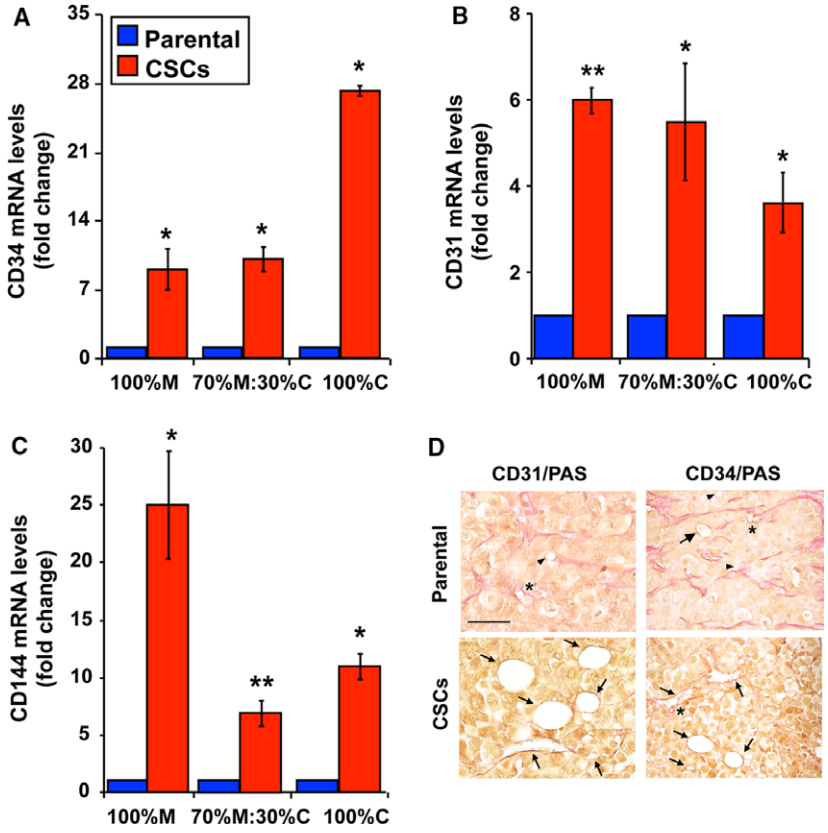

Fig. 3. CSCs have an increased expression of CD34, CD144, and CD31 *in vitro* and *in vivo*. Histograms of CD34 (A), CD31 (B), and CD144 (C) mRNA levels in Parental cells and CSCs cultured on 100% Matrigel, 70% Matrigel:30% collagen I, or 100% collagen I. Real-time PCR values are the means (± SEM) of three independent experiments each performed in triplicate and are reported as fold change relative to Parental cell expression. $*P < 0.05$, $**P < 0.01$. (D) Expression of human CD31 or human CD34 in the tumors described in Fig. 2 was detected by IHC and then counterstained for PAS. Arrows indicate typical vessels positive for PAS and CD31 or CD34, asterisks indicate typical PAS-positive vessels, and the arrowheads indicate vessels negative for both CD31 or CD34 and for PAS.

two groups, high- and low-secreted concentrations. Interestingly, the CSCs had a higher secretion of proangiogenic and growth factors when cultured on Matrigel and their secretion was reduced in a stepwise manner with increasing collagen I concentrations. In particular, the CSCs secreted the proangiogenic factors IGFBP-1, -2, and -3; MCP1; IL8; MMP-9; VEGF; FGF basic (bFGF); epidermal growth factor (EGF); and HGF. On the other hand, among the factors secreted at high levels, we found that, of the more than 50 pro-/antiangiogenic factors screened, the only antiangiogenic factor secreted by the CSCs was Pentraxin 3 (PTX3), and its secretion increased stepwise with increasing collagen I in the ECM.

The secretome profiles for the Parental cells were next measured for cells grown only on 100% Matrigel and 100% collagen I, since those matrices represented the extremes of the changes in the CSC secretome (Fig. 4B). Upon analysis, we found that the Parental cells (a) secreted a higher number of antiangiogenic factors and a lower number of proangiogenic factors than did the CSCs; (b) did not secrete bFGF, EGF, HGF, and MMP9; and (c) secreted all factors at a higher concentration when cultured on collagen I compared to Matrigel, except for VEGF, which was highly secreted from cells grown on Matrigel and decreased when cultured on collagen I (Fig. 4A,B).

The increased expression and activity of VEGFR-2 in CSCs is necessary for VM

As above-reported VEGF, the proangiogenic factor *par excellence* [41] is the only proangiogenic factor secreted by Parental cells and its secretion by CSCs is maximum on Matrigel. We, therefore, hypothesized that the observed CSC vascular phenotype on Matrigel could be activated through autocrine/paracrine loops involving VEGF and VEGFR-2, the receptor mainly associated to tumor angiogenesis [42] [43]. We first measured the VEGFR-2 mRNA levels in cells cultured on ECMs of different compositions compared to its expression in cells cultured in 2D conditions. In the CSCs, VEGFR-2 expression strongly increased in 3D conditions relative to 2D, while VEGFR-2 expression was greatly reduced in the Parental cells compared to 2D (Fig. 5A). To further confirm this expression pattern, we next immunostained sections from subcutaneous tumors produced from either CSCs or Parental cells with human anti-VEGFR-2 (Fig. 5B). To better identify tumor cell-derived vessels, we also

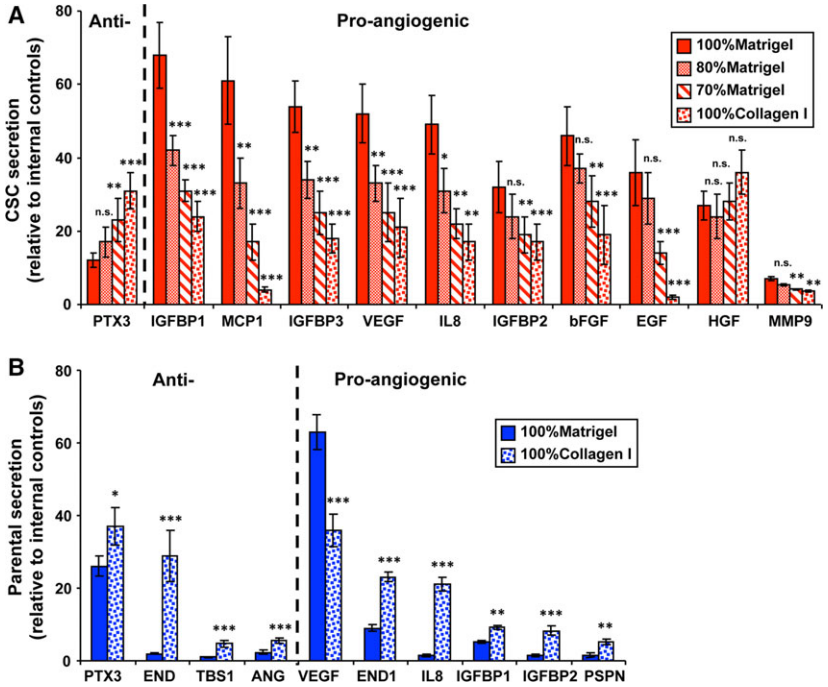

Fig. 4. CSCs release a more proangiogenic secretome compared to the Parental cells and both secretomes are regulated by the ECM composition. (A & B) Secretion profile of anti-, proangiogenic factors, and growth factors secreted by (A) CSCs grown on 100% Matrigel, 80%Matrigel:20% collagen I, 70% Matrigel:30% collagen I, and 100% collagen I; and by (B) Parental cells grown on 100% Matrigel and 100% collagen I. The secretomes from Parental cells and CSCs were subjected to a human angiogenesis antibody array for the simultaneous detection of 55 angiogenesis-related proteins. The spots on each membrane were scanned as digital peaks and the areas of the peaks were calculated in AUs, as described in Materials and methods. Values are the AU means ± SEM of three independent experiments, each performed in duplicate and normalized to the positive controls (reference spots) supplied by the kit. $*P < 0.05$, $**P < 0.01$, $***P < 0.001$ for each protein compared to its secretion on 100% Matrigel.

counterstained with PAS, since VM channels are known to be PAS positive [44]. We found that, compared to the Parental-derived tumors, CSC-derived tumors had a much higher human VEGFR-2 protein expression distributed in PAS-positive VM channels (Fig. 5B). We then functionally determined the role of VEGFR-2 on the basal capacity of the CSCs to form the VM network by incubating the CSCs on Matrigel with the specific VEGFR-2 inhibitor, Ki8751, at 2, 3, 4, or 6 nM Ki8751 for 24 hrs and then analyzing the number of lacunae as described in Methods. As shown in Figures 5C,D, Ki8751 progressively, dose-dependently reduced the VM network while having no effect on CSC growth (data not shown).

Both the secretome and the ECM composition are involved in the reciprocal regulation of growth and morphological plasticity by the CSCs and Parental cells

Given the above-observed cross talk between the two cell lines in regulating the CSC vascular-like phenotype, we next evaluated (a) the effect of each cell line on the growth and morphology of both the opposite cell population and of their same cell population and (b) the role of the ECM composition on these regulatory mechanisms. This was achieved by indirect coculture of the two cell lines for 7 days on the panel of organotypic ECM substrates mirroring PDAC progression (100% Matrigel, 70% Matrigel:30% collagen I, and 100% collagen I). The indirect cocultures were established by collecting the conditioned medium (CM) from either the Parental cell line (Parental-CM) or CSCs (CSC-CM) that had been grown on either 100% Matrigel or 100% collagen I (see protocol schemes in Figs 6A,D and 7A,D and in Materials and methods).

The ECM is involved in the paracrinic inhibition of CSC growth by the Parental secretome but not in the auto-inhibition of Parental growth

We started by analyzing the effects of the Parental secretome (Parental-CM) on growth and morphology

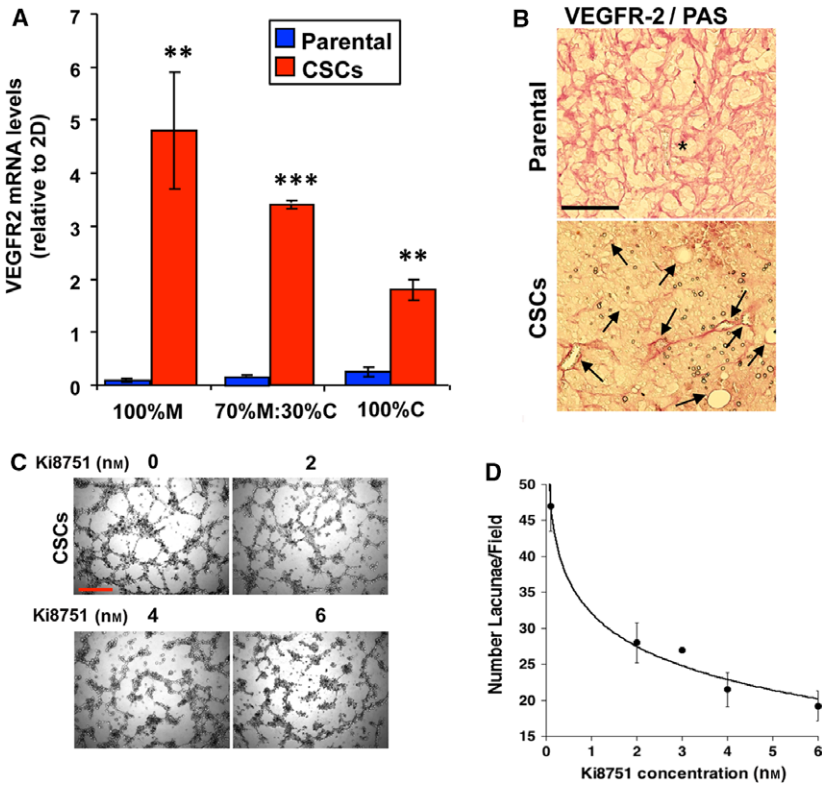

Fig. 5. VEGFR-2 is overexpressed in CSCs, associated *in vivo* with VM and directs basal *in vitro* network formation. (A) Histograms of VEGFR-2 mRNA levels in Parental cells and CSCs cultured on 100% Matrigel, 70% Matrigel: 30% collagen I, and 100% collagen I. Real-time PCR values are the means (± SEM) of three independent experiments each performed in triplicate and are reported as fold change relative to the same cells cultured on cell culture plastic. $^{**}P < 0.01$, $^{***}P < 0.001$. (B) Staining with an anti-human VEGFR-2 antibody of tissue sections from the Parental- and CSC-derived tumors of Fig. 2. Tissue sections were counterstained with PAS. Numerous, large, PAS, and VEGFR-2-positive vessels of human origin are shown in CSC-derived tumors (arrows). The asterisk indicates PAS-positive but VEGFR-2-negative vessels (scale bar, 100 μm). (C & D) Dose response of the specific VEGFR-2 small molecule inhibitor, Ki8751, on the basal *in vitro* ability of the CSCs to form a VM network. (C) Typical images from treatments (scale bar, 500 μm). (D) (IC_{50} = 0.84 ± 0.05 nM, n = 3).

of both CSC (Fig. 6A-C) and Parental cells (Fig. 6D-E) grown on the three different substrates. As can be seen in Figure 6B, Parental secretome, and especially Matrigel-derived Parental-CM (Parental-MCM) reduced CSC growth similarly on all the ECMs (striped bars). Collagen-derived Parental-CM (Parental-CCM, stippled bars) also reduced CSC growth, with even greater inhibitory effects for CSCs growing on ECMs at increasing Matrigel content (100%M and 70%M:30% C). The ECM composition also influenced the Parental secretome-mediated modulation of CSC growth morphology (Fig. 6C,G). Indeed, CSCs grown on 100% Matrigel increased their VM phenotype (Fig. 6C), with an increase in the mean number of closed lacunae following exposition to Matrigel-derived Parental-CM but not to collagen-derived Parental-CM (Fig. 6G). Also the very weak vascular response of the CSCs growing on 70%M–30%C ECM was slightly increased only by the Matrigel-derived Parental-CM (Fig. 6C), which increased the mean number of lacunae compared to nonconditioned cells (Fig. 6G). This is consistent with the previously found Matrigel-induced increase of VEGF secretion by both Parental cells and CSCs and the high VEGFR-2 expression in CSCs when grown on ECM (Fig. 5A) or in CSC-derived subcutaneous tumors (Fig. 5B). For CSCs grown on 100% collagen I, neither Parental-CM induced any apparent changes in CSC morphology with the exception of a tendency for the cells to form cell aggregates instead of a uniform monolayer (Fig. 6C).

We then analyzed the effect of Parental-CMs on Parental cell growth (Fig. 6D). We found that while Matrigel-derived Parental-CM restricted Parental growth almost equally on all substrates (striped bars), the inhibition by the collagen-derived Parental-CM on their own growth increased when collagen I was present in the ECM (stippled bars, Fig. 6E). Furthermore, incubation of the Parental line with either of the CMs

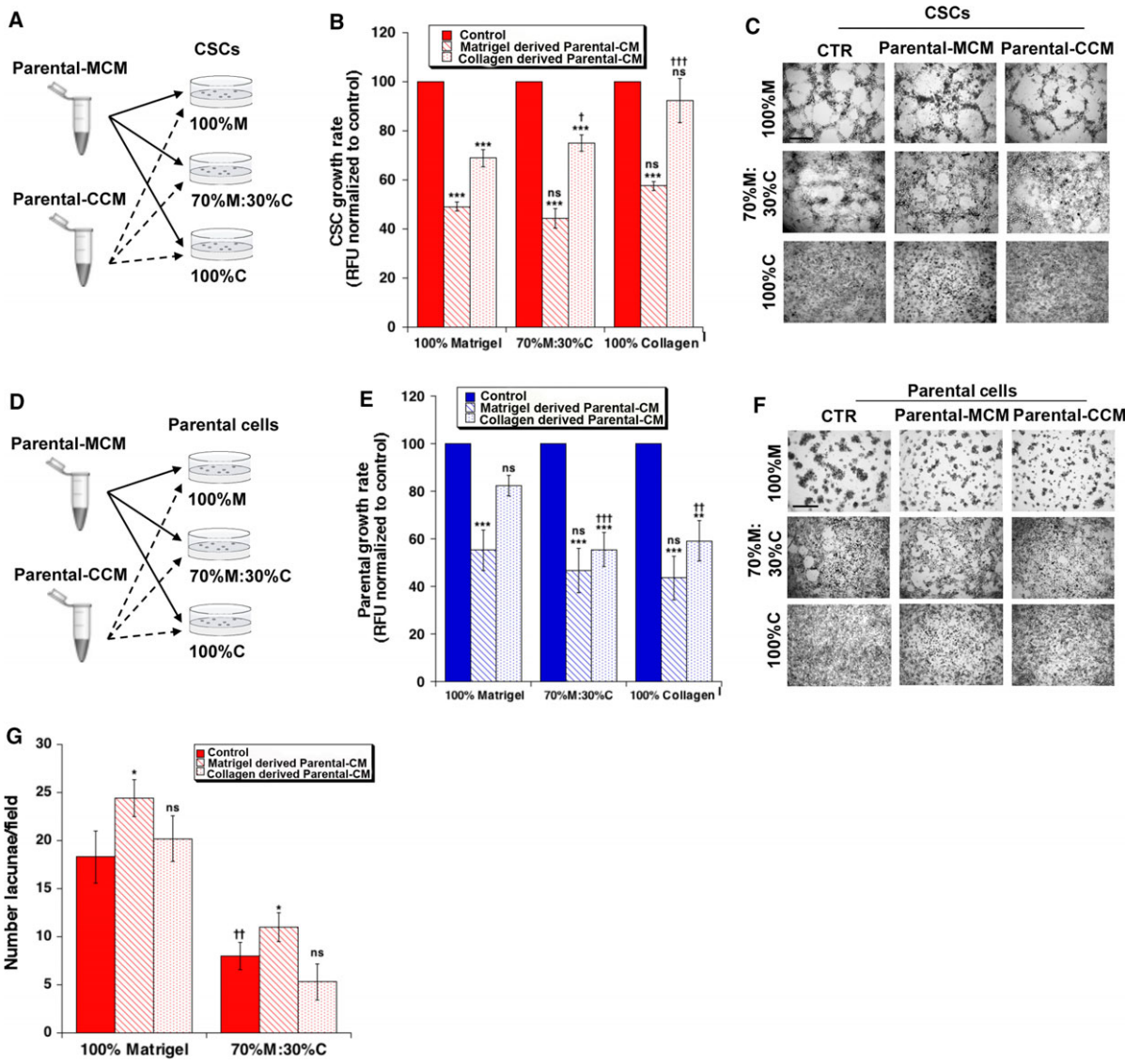

Fig. 6. The Parental secretome paracrinically inhibits CSCs growth especially on Matrigel and autocrinically inhibits their own growth independently of the growth substrate. (A & D) Scheme of the protocol setting used in the indirect coculture experiments to analyze CSCs and Parental cell growth and phenotype. As described in Methods, conditioned medium (CM) that was collected from Parental cells grown on either Matrigel (striped bars; Matrigel-derived Parental-CM) or collagen I (stippled bars; collagen-derived Parental-CM) was used to condition CSCs (A) or Parental cells (D) growing on a panel of organotypic cultures mirroring PDAC progression, from 100% Matrigel (early-stage tumor) to a mixture of 70% Matrigel:30% collagen I (middle-stage tumor) to a substrate of 100% collagen I (high-grade tumor). Growth for CSCs (B) and Parental cells (E) was measured 7 days after the addition of the conditioned media. The Parental secretome paracrinically inhibits CSCs growth especially on Matrigel (B) and autocrinically inhibits their own growth independently of the growth substrate (E). Mean ± SEM, $n = 3$ experiments, ns $P > 0.05$, $^{*}P < 0.05$, $^{**}P < 0.01$, and $^{***}P < 0.001$ compared to each control for each matrix and ns $P > 0.05$, $^{\dagger}P < 0.05$, $^{\dagger\dagger}P < 0.01$, $^{\dagger\dagger\dagger}P < 0.001$ compared to the same CM treatment on 100% Matrigel. Phase-contrast images of CSCs (C) and Parental cells (D) grown on the different ECM compositions and cultured for 7 days as described above. Scale bar represents 500 μm for all images. The Parental secretomes have no effect on their self-phenotype on any substrate composition (F), while the Parental-MCM secretome increases CSC vascular-like morphology when grown on 100% Matrigel and slightly on 70% Matrigel (C). (G) The paracrinic Parental secretome modulates CSC vascular-like channel formation by the CSCs. CSCs were grown on either 100% Matrigel or a mixture of 70%Matrigel/30% collagen I (70%M–30%C) and after 24 hrs to permit their adherence, the cultures were incubated with medium that had been conditioned by Parental cells grown on either 100% Matrigel or 100% collagen I described in Materials and methods. After 7 days in these growth conditions, vascular channel networks were analyzed as described in Materials and methods. Mean ± SEM from three independent experiments, ns (not significant), $^{\dagger\dagger}P > 0.01$ control on 70%M:30%C compared to control on 100% Matrigel; ns, $P > 0.05$, $^{*}P < 0.05$, $^{**}P < 0.01$, $^{***}P < 0.001$ to the control on each matrix.

derived from the Parental cells had no effect on the morphological pattern on any of the three ECM compositions (Fig. 6F).

Altogether these data show that the secretome from Parental cells grown on Matrigel inhibited the growth of both cell types (from 45 to 55%) independently of the ECM composition on which the cells were growing, while the secretome from Parental cells growing on collagen I had a maximum inhibitory effect, respectively, for Parental cells growing on collagen I and CSCs growing on Matrigel.

CSC secretome paracrinically inhibits Parental cell growth and autocrinically stimulates their own growth and vascularity on Matrigel

Simultaneously, we also investigated the effects of the CSC secretomes on Parental and CSC cell growth (Fig. 7B,E) and morphological plasticity (Fig. 7C,F) when cultured on the three different ECMs. The collagen-derived CSC-CM (stippled bars) inhibited Parental growth on Matrigel and this inhibition was reduced as collagen I levels increased, while the Matrigel-derived CSC-CM (striped bars) inhibited Parental cell growth on collagen I and this inhibition was reduced as Matrigel levels increased. That is, the CSC-CMs always blocked Parental growth except when these cells were cultured on the same ECM on which the CSCs had been cultured and the effect of both CMs was intermediate on the cells cultured on 70%M:30%C. Importantly, while both the Matrigel- and collagen I-derived CSC-CMs tended to alter the phenotype of the Parental cells when grown on Matrigel from spheroids toward a very light vascular-like phenotype, they had no effect on the Parental growth morphologies cultured on either the 70%M:30%C ECM or on 100% collagen I. This suggests that changes in growth and plasticity in Parental cells require both ECM-derived and CSC-derived signals.

Interestingly, when the CSC secretome was added to the CSCs themselves, there was a stimulation of only the CSCs growing on Matrigel and exposed to Matrigel-derived CM (Fig. 7E, striped bars) while the growth on the other substrates was either not affected or slightly inhibited by this CM. This suggests the existence of a Matrigel-induced autocrine-positive modulation of CSC growth that could explain the increased CSC propagation on Matrigel observed in Fig. 2B. In contrast, the CSC secretome from collagen I increasingly inhibited their own growth when cultured on increasing concentrations of collagen I (Fig. 7E, stippled bars), suggesting the collagen I-mediated induction of a CSC growth-negative autocrine loop. The ECM composition also influenced the CSC secretome-driven modulation of CSC growth morphology (Fig. 7F,G). Indeed, the CSCs tendency to organize in a vascular-like network, with anastomosed tube-like structures forming lacunae, when cultured on Matrigel was strongly autocrinically increased after their incubation with the Matrigel-derived CSCs-CM and somewhat increased by the collagen-derived CSC-CM (Fig. 7G). Furthermore, incubation with the Matrigel-derived CSC-CM also slightly increased the weak tendency of CSCs cultured on the 70%M–30%C ECM to generate lacunae (Fig. 7G). The collagen-derived CSC-CM did not induce any apparent changes in CSC growth morphology when grown on 100% collagen I.

VEGFR-2 mediates the autocrinic and paracrinic stimulation of CSC VM on Matrigel

The above data show that CSCs grown on 100% Matrigel increased their VM phenotype with an increase in the mean number of closed lacunae following exposition to Matrigel-derived CM from either Parental cells (Fig. 6C,G) or CSCs (Fig. 7C,G). This together with fact that only VEGF secretion was stimulated by Matrigel in both cell lines (Fig. 4) and the high VEGFR-2 expression in CSCs when grown on 3D (Fig. 5A) suggests that the autocrinic and paracrinic stimulation of CSCs vascularity (VM) on Matrigel was due primarily to the VEGF activation of VEGFR-2. In support of this hypothesis, the specific VEGFR-2 inhibitor, Ki8751, blocked the increased CSC vascular response on 100% Matrigel due to Matrigel-derived CM from both Parental cells and CSC (Fig. 8A,B). Interestingly, this inhibition was stronger in the MCM than in the basal, control conditions.

Discussion

Human PDAC is composed of heterogeneous cell populations including tumor (parenchymal, CSCs) and stromal populations (fibroblasts, immune, and endothelial cells) embedded in an extensive collagen I-rich fibrotic ECM, known as desmoplasia. This desmoplastic ECM creates a dynamic, tumor-supportive microenvironment by actively modulating key signaling events promoting tumor growth and invasion. Unlike most other tumors, desmoplasia is a characteristic hallmark of PDAC and becomes more abundant as the tumor progresses. Indeed, only minimal fibrosis is observed in the relatively normal pancreas [34], while an increased collagen I expression in the human PDAC stroma is associated with increased metastasis

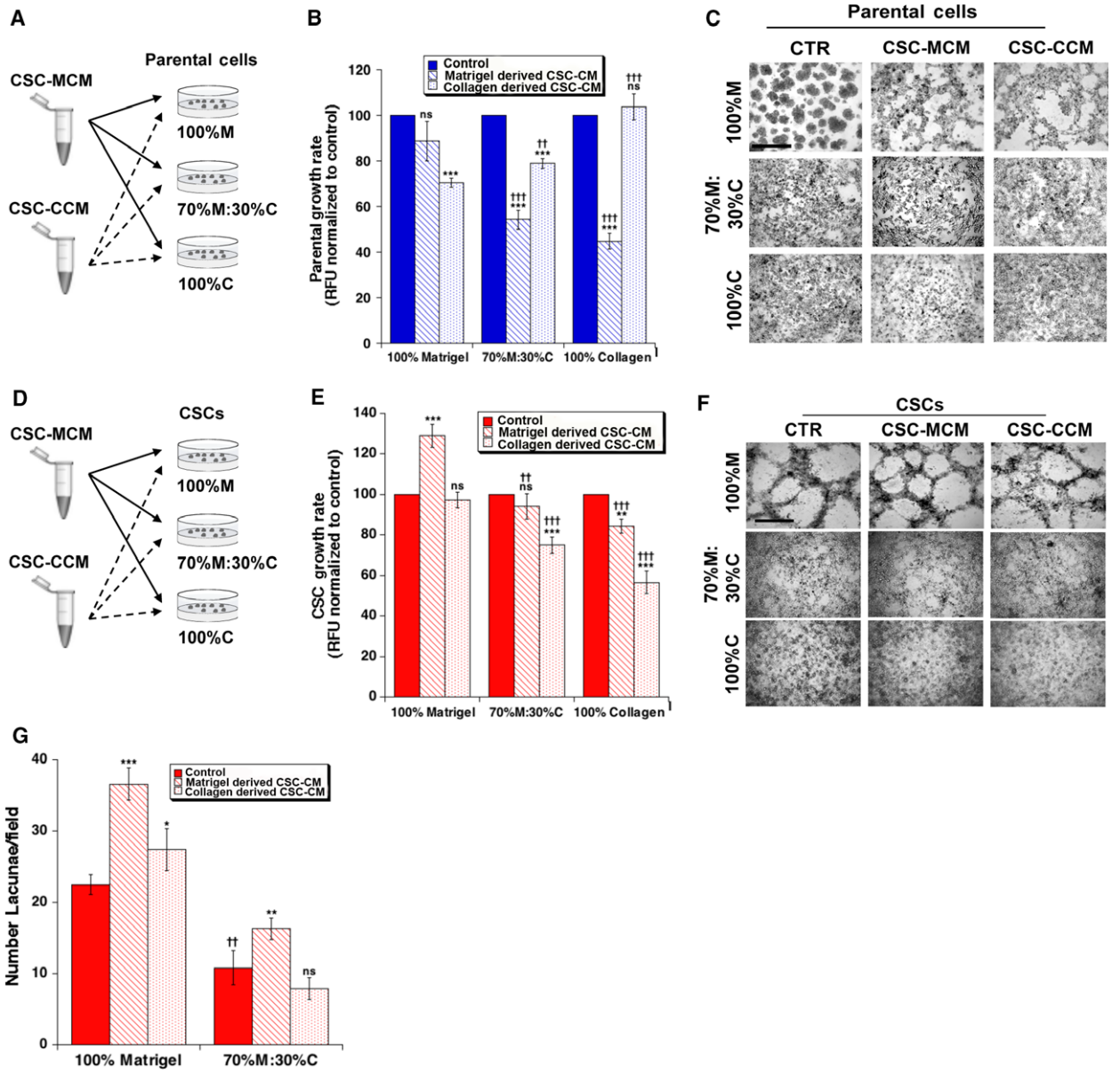

Fig. 7. ECM composition modulates the paracrinic and autocrinic regulation of cell growth and morphology by the CSC secretome. (A & D) Scheme of the protocol setting used in the indirect coculture experiments to analyze CSCs and Parental cell growth and phenotype as described in Fig. 4. The CSC secretomes paracrinically inhibit Parental cell growth only on the opposite ECM from which it was collected (B). The Matrigel-derived CSC-CM autocrinically stimulates CSC growth on Matrigel and slightly inhibits CSC growth on the other substrates while collagen-derived CSC-CM has an increasing inhibitory effect on CSC growth as collagen I content increases (E). Data represent mean ± SEM from three independent experiments, ns, $P > 0.05$, $^{*}P < 0.05$, $^{**}P < 0.01$, $^{***}P < 0.001$ and ns, $P > 0.05$, $^{\dagger}P < 0.05$, $^{\dagger\dagger}P < 0.01$, $^{\dagger\dagger\dagger}P < 0.001$ compared to the same CM treatment on 100% Matrigel. Phase-contrast images of Parental cells (C) and CSCs (F) grown on the different ECM compositions and cultured for 7 days with their growth medium or with either the CSC-MCM or the CSC-CCM. Scale bar represents 500 μm for all images. CSCs secretome stimulates the vascular-like morphology of both Parental cells (C) and CSCs (F) grown on Matrigel. (G) The autocrinic CSC secretome modulates CSC vascular-like channel formation by the CSCs. CSCs were grown on either 100% Matrigel or a mixture of 70%Matrigel/30% collagen I (70%M–30%C) and after 24 hrs to permit their adherence, the cultures were incubated with medium that had been conditioned by CSCs grown on either 100% Matrigel or 100% collagen I as described in Materials and methods. After 7 days in these growth conditions, vascular channel networks were analyzed as described in Materials and methods. Mean ± SEM from three independent experiments, ns (not significant), $^{\dagger\dagger}P > 0.01$ control on 70%M:30%C compared to control on 100% Matrigel; ns, $^{*}P < 0.05$, $^{**}P < 0.01$, $^{***}P < 0.001$ to the control on each matrix.

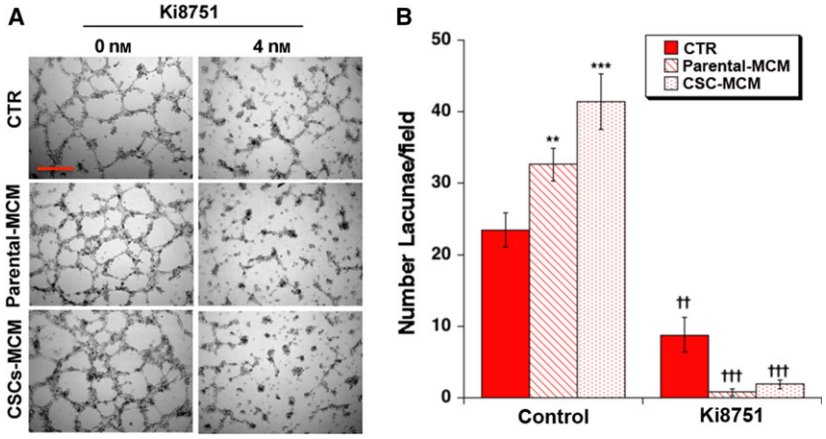

Fig. 8. Inhibition of the VEGFR-2 blocks the stimulation of the CSC vascular phenotype by Matrigel conditioned medium (MCM). CSCs were plated on 100% Matrigel and after 24 hrs to permit their adherence the cultures were incubated with medium that had been conditioned by Parental cells or CSCs grown on 100% Matrigel with either vehicle or 4 nM of the VEGFR-2 inhibitor, Ki8751. After 24 hrs, vascular channel networks were analyzed as described in Materials and methods. (A) Typical images from the experiments (scale bar, 500 μm) and (B) the number of lacunae counted per field at 2X; mean ± SEM from three independent experiments, $^{**}P < 0.01$, $^{***}P < 0.001$ of each CM treatment compared to the control in the medium without Ki8751 and $^{\dagger\dagger}P > 0.01$, $^{\dagger\dagger\dagger}P > 0.001$ of each CM containing Ki8751 compared to its CM without Ki8751.

and poor prognosis [45]. Furthermore, during PDAC progression, the normal laminin-rich basal membrane architecture is disrupted and tumor cells are directly exposed to interstitial collagen, which enhances tumor progression (for review [9]). For this reason, it is important to develop representative culture models of the tumor ECM conditions mimicking the stromal changes observed during the *in vivo* PDAC progression from a laminin-rich to a collagen I-rich environment. For this, we generated a series of 3D organotypic culture platforms by using matrices composed of 100% Matrigel, a laminin-rich extract of a basement membrane representing a stromal microenvironment at the initial phases of tumor development, plus increasing concentrations of collagen I up to 100% collagen I.

Using these culture platforms, we characterized the role of the ECM composition on the level of tumor stemness (Fig. 1), and growth rate, morphology, and invasiveness of the Panc1 Parental cells and their derived CSCs (Fig. 2), their *in vitro* and *in vivo* endothelial marker expression (Fig. 3), their angiogenic/growth factor secretome (Fig. 4), *in vitro* and *in vivo* VEGFR2 gene expression (Fig. 5) and, finally, the dynamics of the interaction of the two cells types in indirect coculture on the different ECMs (Figs 6 and 7) and the role of VEGF/VEGFR-2 in this interaction (Fig. 8). We find that changes in the ECM composition resulted in differences between Parental cells and CSCs in all these characteristics.

In particular, we found that when grown on Matrigel-enriched organotypic culture, the morphology of the CSCs was altered to elongated, mesenchymal-like cells and formed tube-like structures resembling VM (Fig. 2A). Furthermore, they overexpressed the CSC marker CD44v6 (Fig. 1A), which has been associated with an increased VM ability [46]. On the other hand, on organotypic cultures rich in collagen I, which dominates the ECM of an advanced PDAC tumor [28], the CSC's VM was shifted to a typical epithelial-like phenotype with cells growing as a monolayer (Fig. 2A) and expressing the highest levels of E-cadherin in 3D culture (Fig. 1B). In contrast, Parental cells on Matrigel grew as spheroid-like colonies that reprogrammed their phenotype into a monolayer-like tissue as the collagen I content in the ECM increased (Fig. 2A). These effects of ECM on Parental cell and CSC morphological phenotypes were also found in two other PDAC cells lines, MiaPaCa2 and PSN1, suggesting that the observed phenomenon is general and not limited to a unique cell line (data not shown). This observed vascular/mesenchymal to epithelial phenotypic shift, driven by the different ECM compositions, reflects the known high plasticity reported for PDAC in particular [47] and for CSCs in general [48] and has emerged in this study as a typical marker of the CSC lineage. We hypothesize that the CSC's acquisition of the VM phenotype when grown on an early tumor ECM (Matrigel) contribute to the tumor vascularization, which is necessary for tumor initiation and the recruitment of nutrients particularly at the initial phases of tumor development [49]. Indeed, it is already known in several tumor types that CSCs highly express the

endothelial cell markers CD34 [50–52], CD144 (VE-cadherin) [53], and CD31 [54] and are able to differentiate into endothelial cells, thus contributing to tumor vascularization and growth [55]. Here, we observed that the PDAC CSCs already highly expressed the mRNAs encoding for CD34, CD144, and CD31 with respect to their Parental counterpart in 2D cultures and this endothelial-like mRNA signature was retained by CSCs when propagated in 3D cultures (Fig. 3A). Consistent with this, tumor sections derived from the subcutaneous transplantation of CSCs in nude mice contained increased vessel density and blood perfusion and showed a higher number of both PAS+ and human CD34 + /CD31 + blood vessels compared to the Parental cell-derived tumors (Fig. 3B). This suggests that also in PDAC, such as in other tumor types, CSCs, having a high degree of differentiation plasticity, can transdifferentiate in endothelial-like cells to contribute to tumor vascularization. Moreover, in line with their higher capacity to express endothelial-like markers, we also found that the CSCs' ability to promote the development of a 'cancer vascular niche' [56] was also due to their secretion of proangiogenic factors. Indeed, when grown on Matrigel CSCs released a proangiogenic secretome (Fig. 4A) having very high levels of IGFBP-1, -2, and -3, MCP-1, VEGF, and IL8, as well as of growth factors known to support both tumor growth and angiogenesis (e.g., EGF, HGF, and FGF basic). Importantly, the secretion of this plethora of angiogenic factors was maximal when cells were on Matrigel and was reduced stepwise with increasing collagen I concentrations.

In contrast to CSCs, we found that Parental cells, in line with their inability to form tube-like structures on either Matrigel or collagen I, secreted a higher number of antiangiogenic factors and these were up-regulated when they grew on collagen I. Importantly, the only factor to have an increased secretion on Matrigel was VEGF, the proangiogenic factor *par excellence* known to stimulate vasculogenesis and angiogenesis through both autocrine and paracrine mechanisms [57]. Indeed, VEGF was secreted from Parental cells at the same level as in CSCs (Fig. 4B). In line with this, on all substrates (a) the CSCs greatly overexpressed the mRNA for its receptor VEGFR-2 in comparison to 2D, while Parental cells decreased their VEGFR2-mRNA levels compared to 2D (Fig. 5A); (b) had much higher VEGFR-2 expression *in vivo* (Fig. 5B); and (c) lost their ability to form vascular networks on Matrigel when VEGFR-2 activity was blocked with its specific inhibitor, Ki8751 (Fig. 5C).

Based on these findings, CSCs could develop their vascular phenotype on Matrigel by virtue of two interacting and coordinated factors: (a) the intrinsic overexpression of genes for endothelial factors and vascular receptors and (b) the very high secretion of numerous proangiogenic/growth factors which support their high growth rate in order to form the vascular network. This would both mobilize CSCs (together with endothelial cells, pericytes, etc.) into a vascular niche and further stimulate the CSCs endothelial-like differentiation program, in order to participate in VM, and their angiogenic secretome to stimulate endothelial angiogenesis [49]. This enhanced ability of CSCs to activate a growth/proangiogenic program, especially in response to an early-stage tumor microenvironment (e.g., growth on Matrigel), explains our *in vivo* experiments in which (a) the subcutaneous tumors originating from CSCs gave rise to a more abundant vascular network composed of larger vessels than the tumors originating from Parental cells (Fig. 2F, left panel, 3D and 5C) and (b) the tumors of the CSC-injected mice had increased Ki-67 staining for mitotic index (Fig. 2F, right panel) and grow faster than those in mice injected with Parental cells [14].

This last finding reflects the CSCs' enhanced *in vitro* growth rate compared to Parental cells when the two cell lines were cultured on Matrigel-organotypic cultures (Fig. 2B) and further validates the use of our organotypic cultures as biomimetic *in vitro* models of the *in vivo* tumor biology. The data also suggest a link between the very low percentage of CSCs (< 1%) found in human PDAC tissues [58] and the known hypovascular and collagen I-rich nature of pancreatic cancers. Indeed, in our collagen I-rich organotypic cultures, mimicking an advanced PDAC, CSC growth was reduced compared to that on Matrigel to a level similar to Parental cell growth (Fig. 2B) on the other ECMs and, analogously to Parental cells, displayed a nonendothelial-like phenotype (Fig. 2A).

However, tumor growth rate and phenotype is influenced not only directly via intrinsic (gene expression-related) and extrinsic (ECM-related) factors but also via the secretion of soluble factors inducing autocrine and paracrine growth regulating loops. Therefore, we also analyzed in indirect cocultures (via their respective secretomes released into the CM), the dynamics of the autocrinic and paracrinic growth regulation when the two cell types were cultured on the different ECM compositions (see protocol schemes in Fig. 6A,D and 7A,D). We found that when the two cell populations were cultured on a Matrigel-enriched substrate (upper part of model in Fig. 9), Parental cells derived secretome (Parental-MCM) both paracrinically inhibited CSC growth and autocrinically inhibited their own growth (Fig. 6B,E), while the CSC-derived secretome (CSC-MCM) enhanced their own growth (Fig. 7E,

stippled bars) and had a slight inhibitory effect on the growth of the Parental cells (Fig. 7B, stippled bars). Thus, the Parental-CSC coexistence on Matrigel would result in a significant increase of CSC growth compared to Parental growth (upper part of model in Fig. 9). This confirms both the overturning of the 2D Parental and CSC growth rates when grown on Matrigel (Fig. 2B) and the *in vivo* experiments with both subcutanous (Ki67, Fig. 2F) and direct spleen injection [14]. Furthermore, the CSCs through their complex Matrigel-induced proangiogenic secretome (Fig. 4A) and, partially, via the Parental cell secretion of VEGFA (Fig. 4B), stimulated the VEGFR2-overexpressing CSCs (Fig. 5A) to an increased vasculogenic phenotype (VM) when these cells were cultured on Matrigel-rich ECMs (Figs 6C,G and 7F,G). When the two cell lines were indirectly cocultured on collagen I (lower part of model in Fig. 9) and in line with their reduced secretion of growth/angiogenic factors secreted on this ECM (Figs. 4A & B), they autocrinically inhibited themselves (Figs 6E and 7E), while having no paracrinic effect on the opposite cell subpopulation (Figs 6B and 7B). Consequently, on collagen I, both Parental and CSCs had restricted growth programs as was found in Fig. 2B.

In conclusion, our study sheds light on one of the most representative PDAC hallmarks, i.e., the very early development of metastasis even before the primary tumor can be detected [18]. Indeed, when growing on an early tumor ECM, dominated by laminin, collagen IV, and entactin (modeled by the Matrigel ECM), the CSCs are dedicated toward the preparation of a vascular niche by secreting high levels of proangiogenic/growth factors which activate their growth program, their assembly into a VEGF/VEGFR-2-mediated VM network (Fig. 2A), and eventually their transdifferentiation into an endothelial-like network (Fig. 3D). At the same time, when on Matrigel, the more differentiated parenchymal tumor cell population has a reduced growth rate (Fig. 2B) but with a

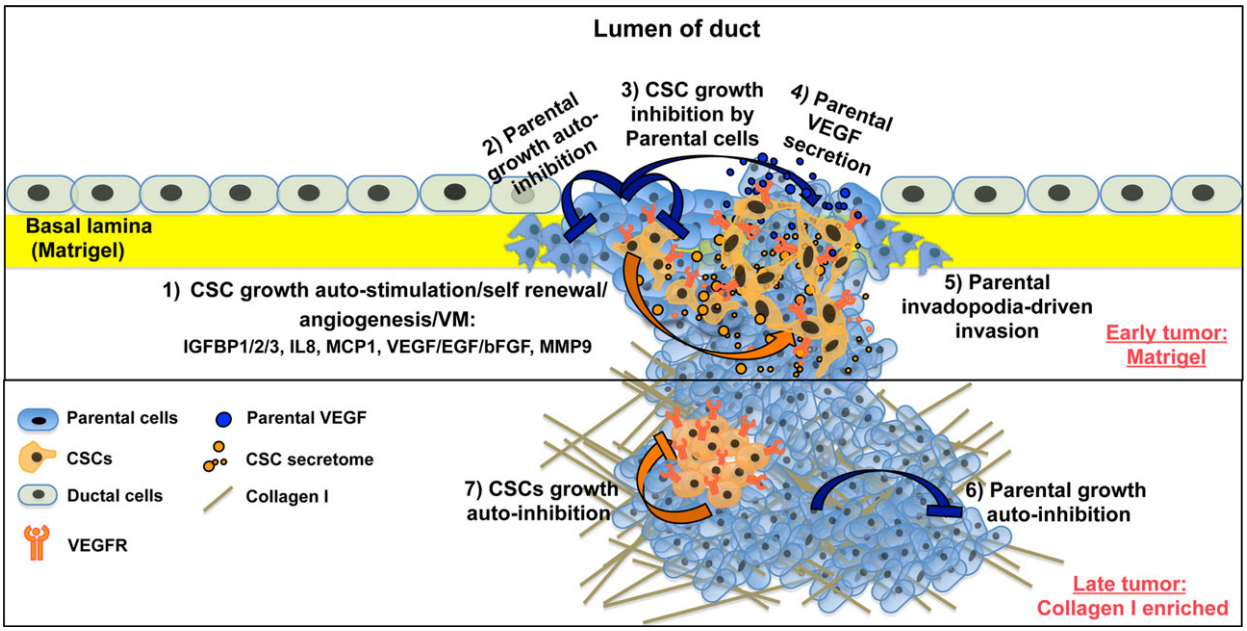

Fig. 9. Model of Influence of the ECM composition on the autocrine regulation of Parental and CSC growth and plasticity and their paracrine cross talk via their angiogenic secretome. Matrigel induces the formation of autocrine loops in CSCs. Indeed, on Matrigel (1) CSCs secrete a high amount of potent proangiogenic and growth factors (IGFBP1/2/3, MCP1, IL8, EGF, VEGF, and bFGF), which, via autocrine mechanisms, stimulate their growth/self-renewal and their intrinsic vascular-like propensity/traits/potential such that they rapidly expand forming vascular-like structures and thus contributing to the vascular phenotype of the early-stage tumor. However, on Matrigel, the Parental cells (2) auto-inhibit their growth and (3) restrict the CSC's growth while (4) also supporting the CSC's vascular-like phenotype via a paracrine activity, which involves both a high level of VEGF secretion by Parental cells and VEGFR-2 overexpression by the CSCs. While the CSCs express the proangiogenic genes CD31, CD34, and CD144, they are able to produce the angiogenic switch only on substrates that (i) increase the expression of VEGFR-2 and (ii) stimulate the secretion of high enough levels of proangiogenic factors to push the cells into the vasculogenic program. Growth on Matrigel also stimulates the Parental cell invasion program through activation of invadopodia (5). Lastly, the development of the desmoplastic stroma during progression, resulting in higher levels of collagen I, restricts the growth of both Parental cell (6) and CSCs (7) via autocrine loops.

high-invadopodia-driven invasive capacity (Fig. 2D,E) that is stimulated by EGF [32], which is highly secreted by the CSCs (Fig. 4A). This concerted activation of these two malignant phenotypes, i.e., (a) the high rate of local invasion executed by parenchymal cells into the (b) aberrant vascular network created by the CSC-derived vascular signals suggest that a symbiotic relationship between the parenchymal cells and the CSCs underlies the initiation and maintenance of early PDAC infiltration and metastasis.

Materials and methods

Cell lines

The Panc1 human pancreatic adenocarcinoma Parental cell line was grown in RPMI 1640 supplemented with 10% FBS, 2 mM glutamine, and 50 $\mu g \cdot mL^{-1}$ gentamicin sulfate (Gibco, Life Technologies). Panc1 cells are mutated in the PDAC driver genes KRAS, CDKN2A, MAP2K4, and TP53 [29] and are a well established and widely used model in PDAC research [59]. Adherent cells were maintained in standard conditions for a few passages at 37° C with 5% CO_2. Panc1 CSCs were generated as previously described [14] and cultured in CSC medium, i.e., Dulbecco's modified Eagle's medium (DMEM)/F-12 without glucose (US biological Life Sciences) supplemented with 1 $g \cdot L^{-1}$ glucose, B27 serum substitute (Gibco, Life Technologies), 1 $\mu g \cdot mL^{-1}$ Fungizone (Gibco, Life Technologies), 1% penicillin/streptomycin (Gibco, Life Technologies), 5 $\mu g \cdot mL^{-1}$ heparin (Sigma), 20 $ng \cdot mL^{-1}$ EGF (Peprotech), and 20 $ng \cdot mL^{-1}$ FGF (fibroblast growth factor, Peprotech).

CSCs were selected on the basis of their dynamic equilibrium with the rest of the tumor cells and their property to be enriched and selected for when grown in the above-described conditions. The CSCs were selected from the PDAC cell line Panc-1 (the Parental line) and identified by their ability to form anchorage independent colonies and by their overexpression of common CSC markers [14].

3D culture models

100% Matrigel

Matrigel (Corning Matrigel Growth Factor Reduced Basement Membrane Matrix, Phenol Red-Free) was thawed on ice. Matrigel was diluted at the final concentration of 7 $mg \cdot mL^{-1}$ in RPMI 1640 without gentamicin sulfate and without FBS.

100% collagen I

Collagen I bovine (Gibco, Life Technologies) was diluted at the final concentration of 3 $mg \cdot mL^{-1}$ in sterile water, PBS 10X (Sigma Aldrich), and 0.015 N NaOH.

The various mixtures of Matrigel and collagen I were prepared at final concentrations based on the dilution of the above final concentrations of Matrigel and collagen I:

90% Matrigel-10% collagen I

The mixtures of Matrigel and collagen I were prepared at the final concentration of 6.3 $mg \cdot mL^{-1}$ and 0.3 $mg \cdot mL^{-1}$, respectively, as described above and then mixed.

80% Matrigel-20% collagen I

The mixtures of Matrigel and collagen I were prepared at the final concentration of 5.6 $mg \cdot mL^{-1}$ and 0.6 $mg \cdot mL^{-1}$, respectively as described above and then mixed.

70% Matrigel-30% collagen I

The mixtures of Matrigel and collagen I were prepared at the final concentration of 4.9 $mg \cdot mL^{-1}$ and 0.9 $mg \cdot mL^{-1}$, respectively as described above and then mixed.

20% Matrigel-80% collagen I

The mixtures of Matrigel and collagen I were prepared at the final concentration of 1.4 $mg \cdot mL^{-1}$ and 2.4 $mg \cdot mL^{-1}$, respectively as described above and then mixed.

In all cases, 500 μL of the mixture was plated in 24-well cell culture plates. The cell culture plates were then incubated at 37° C with 5% CO_2 for 1 h in order to allow the mixture to create a thin gel on the bottom of the wells. About 8.8×10^5 cells/well were seeded on the top of the matrix and incubated at 37° C with 5% CO_2 for 5 days. Medium was changed every 2 days.

3D matrix digestion for cell recovery

100% Matrigel

CellSperse (DIVAA, Trevigen) is a bacillus-derived neutral metalloprotease that was used to recover cells from the matrix composed by Matrigel. Briefly, two volumes of CellSperse were added in each well and incubated at 37° C with 5% CO_2 for 2 h. One volume of 10 mM EDTA was added to stop CellSperse reaction and cells were centrifuged at 400 ***g*** for 5 min. Cells were then washed twice with one volume of PBS and centrifuged at 2000 r.p.m. for 5 min and at 16 000 ***g*** for 2 min, respectively.

100% collagen I

Collagenase type I (Gibco, Life Technologies) was used to recover cells from the matrix composed by collagen I. Briefly, one volume of the prewarmed collagenase solution was

added to completely submerge the portion of the gel to be digested and was incubated at 37° C with 5% CO_2 for 2 h. Two volumes of medium containing serum (RPMI 1640 and DMEM/F-12 for the Parental cell line and for the CSCs, respectively) were added to stop collagenase reaction. Cells were centrifuged at 400 ***g*** for 5 min, washed with one volume of PBS and centrifuged at 400 ***g*** for 5 min.

For the various mixtures of Matrigel and collagen I

The matrix was digested using both CellSperse and collagenase solution as described above.

Growth measurements

Curves of Parental cells and CSCs cultured on the different ECMs were calculated from cell growth measured by Resazurin (Immunological Sciences, Rome, Italy) reduction assays as previously described [27] where 10 μL stock Resazurin was added to 100 μL medium and fluorescence was measured after 3 h. Cell numbers were calculated according to the standard curves obtained by fluorescence readings of Resazurin on serial dilutions of both Parental cells and CSCs. Parental and CSC doubling times (Td) were calculated from each growth curve as previously described [27].

Invadopodia proteolytic activity

Invadopodia focal ECM proteolysis experiments were conducted in cells seeded onto a layer of either Matrigel (diluted to a final concentration of 4 $mg{\cdot}mL^{-1}$) or 80% collagen I:20% Matrigel (2.4 $mg{\cdot}mL^{-1}$ collagen I and 1 $mg{\cdot}mL^{-1}$ Matrigel) in which quenched BODIPY linked to BSA (DQ-Green-BSA and DQ-Red-BSA) was mixed at a final concentration of 30 $\mu g{\cdot}mL^{-1}$. The matrix mix was used to cover 12-mm round glass coverslip. Then, 4×10^4 cells/coverslip were seeded onto the polymerized matrix, and grown overnight. Cells were then fixed with paraformaldehyde 3.7% in PBS and processed for immunofluorescence. Focal ECM digestion produces green fluorescence within a black background. Cells were imaged for F-actin and quantification of ECM degradation was done by counting degradation spots in 10 fields of view (40 × objective) in five separate experiments for each cell line. The degradation area was determined by using ImageJ 1.41 software and normalized for the number of cells. ECM degradation was analyzed as total focal digestive activity of 100 cells (Digestion Index) and standardized to 100% for Parental cell activity.

Invasion measurements

A quantitative measure of the degree of *in vitro* cellular invasion was measured as the ability to traverse an 8 μm polycarbonate membrane coated with 100% Matrigel (5 $mg{\cdot}mL^{-1}$) or 80% collagen I:20% Matrigel (2.4 $mg{\cdot}mL^{-1}$ collagen I and 1 $mg{\cdot}mL^{-1}$ Matrigel) and placed in Boyden chambers. The cells were then trypsinized, and 200 000 tumor cells were added in suspension to the upper chamber of the Boyden chamber in which the lower chamber contained 1% serum in culture medium. Culture dishes were returned to the incubator for 24 h, and then the filters were removed from the chamber, fixed, and strained with the Diff-Quik Stain Kit (Baxter Diagnostics). The cells that had not traversed the filter were delicately removed with a q-tip and cells that had traversed the filter were counted in 10 fields in 20 × for each treatment and cell type.

RNA extraction and qPCR

Cells were recovered from each ECM as described in section 2.3 and total RNA was extracted using TRIzol Reagent (Life Technologies) and 1 μg of RNA was reverse transcribed using first-strand cDNA synthesis. Real-time quantification was performed in triplicate samples by SYBR Green detection chemistry with Power SYBR Green PCR Master Mix (Applied Biosystems) on a 7900HT Fast Real-Time System (Thermo Fisher). The primers used were: E-cadherin forward, 5′-GAC ACC AAC GAT AAT CCT CCGA-3′ and reverse, 5′-GGC ACC TGA CCC TTGTAC GT-3′; CD44v6 forward, 5′-AGG AAC AGT GGT TTG GCA AC-3′ and reverse, 5′-CGA ATG GGA GTC TTC TCT GG-3′; ribosomal protein large P0 (RPLP0) forward, 5′-ACA TGTTGC TGG CCA ATA AGG T-3′ and reverse, 5′-CCT AAAGCC TGG AAA AAG GAG G-3′. CD31 forward 5′-GCA ACA CAG TCC AGA TAG TCG T-3′ and reverse 5′-GAC CTC AAA CTG GGC ATC AT-3′; CD34 forward 5′-GCG CTT TGC TTG CTG AGT-3′ and reverse 5′-GGG TAG CAG TAC CGT TGT TGT-3′; CD144 forward 5′-GAA CCC AAG ATG TGG CCT TTA G-3′ and reverse 5′-GAT GTG ACA ACA GCG AGG TGT AA-3′; VEGFR2 forward 5′-GCA GAG CCA TGT GGT CTC TCT GG-3′ and reverse 5′-TGG CGC ACT CTT CCT CCA ACT GC-3′.

The following cycling conditions were used: 95° C for 10 min, 40 cycles at 95° C for 15 s, 60° C for 1 min, and 72° C for 30 s. The average of cycle threshold of each triplicate was analyzed according to the $2^{(-\Delta\Delta Ct)}$ method.

Human Angiogenesis array

For the analysis of secreted angiogenic growth factors, 1.5×10^5 cells/well were seeded on each of the ECM compositions in 24-well cell culture plates. Medium was changed every 3 days. When the monolayer reached approximately 80% confluence, they were incubated with 1 mL of medium without FBS, growth factors, or antibiotics for 30 h. The conditioned media (CM) were

collected, centrifuged, and the protein concentration was measured for each with the Bradford protein assay reagent (Pierce, Milan, Italy) using bovine serum albumin as a standard. Each sample was prepared at 40 μg protein in a final volume of 1.5 mL, collected in new tubes and frozen at −80 °C until use and then defrosted and kept on ice. The 'Human Angiogenesis Array' Kit was purchased from the R&D systems (Minneapolis, MN, USA) for the detection of 55 protein associated with human angiogenesis. The Detection Antibody Cocktail was added in each sample for 1 h at room temperature and the samples were loaded on the array membranes and incubated overnight at 4° C on a rocking platform. Then, 1.5 mL of streptavidin-HRP solution (1 : 2000) was then added onto each membrane. For immune-detection, each membrane was incubated with Pierce ECL Western blotting substrate (ThermoFisher scientific, Waltham, MA USA) and was exposed to X-ray film for different times to obtain a range of exposures from very short exposure for the highly expressed factors to medium and longer exposures to visualize the medium and low expressers. Array data on developed X-ray film were quantitated by scanning as digital peaks and the areas of the peaks were calculated in arbitrary units (AU) using the public domain NIH IMAGE software (http:rsb.info.nih.gov/nihimage/) and values were normalized to the positive control reference spots supplied by the kit. A cutoff of 1 as the lower value for the AU was applied.

Indirect coculture studies

Conditioned medium (CM) was prepared as above and stored in liquid nitrogen. To condition cells, both Parental and CSCs were grown for 1 day on 100%M, 70%M/:30% C, or 100%C in their corresponding complete culture media and for the subsequent 5 days in their same complete culture media diluted at 50% with the CMs collected from either the Parental cells on Matrigel (Parental-MCM) and collagen (Parental-CCM) or from the CSC on Matrigel (CSC-MCM) and collagen I (CSC-CCM). A change of medium was conducted midweek. To analyze if the CMs could change the growth and/or the growth phenotype (morphology) of the cells, growth was assessed by the Resazurin cell viability assay and morphology was examined microscopically.

As serum (or B27 for CSCs) contains growth factors, cytokines, and chemokines, we performed preliminary experiments with the CMs in the absence of serum, in order to examine the direct effect of the CMs on the growth of each cell population without serum-mediated interferences. As a comparison, we conducted the same experiments in the presence of 5% and 10% of serum/B27. As we found similar trends compared to relative controls for the biological functions (growth and morphology) under the different serum/B27 concentrations, we conducted all the subsequent growth experiments with CMs in 5% serum/B27-containing growth media.

Vascular network analysis

CSCs were grown on either 100% Matrigel or a mixture of 70%Matrigel/30% collagen I (70%M–30%C) and after 7 days in these growth conditions, vascular channel networks were photographed using the TE200 microscope (Nikon USA, Garden City, NY, USA). Vascular channels were quantified by measuring as a morphometric parameter the number of internal lacunae (i.e., the empty regions of the field delimited by tubules and cell clusters) per microscope field (20X). At least five randomly chosen low-power fields were counted per sample and the number of closed lacunae was counted for each treatment. To study autocrine or paracrine regulation, CSCs were cultured as above and after 24 hrs to permit their adherence, the cultures were incubated with medium that had been conditioned by either Parental cells or CSCs that had been grown on either 100% Matrigel (Matrigel-derived CSC-CM) or 100% collagen I (collagen-derived CSC-CM) as described above for indirect coculture. The effect of the specific VEGFR-2 inhibitor, Ki8751, on vascular network formation was determined by incubating the CSCs on Matrigel with 2, 3, 4, or 6 nM Ki8751 for 24 hrs and then analyzing the network as above. Its effect on autocrine or paracrine regulation was determined by adding 2 nM Ki8751 in the conditioned medium.

Subcutaneous *in vivo* model

Animal studies were approved by the Verona University Review Board and by the Italian Ministero della Salute. About 1×10^5 Panc1 Parental cells or CSCs were injected subcutaneously into the dorsal flank of five nude female mice (5 weeks of age, Charles River). Animals were sacrificed when the volume of the tumor reached 2 cm^3 and, immediately after death, neoplastic masses were collected for histological assessment. To perform histological analysis, tissue samples were fixed in 10% (vol/vol) neutral-buffered formalin for 24–48 h and were processed routinely. Serial histological sections (4–6 μm thick) were obtained from each paraffin block and stained with the Masson's trichrome stain or PAS stain for ECM collagen and ECM glycoproteins, respectively. Immunohistochemistry (IHC) was performed as described below.

Immunohistochemistry

The sections (5 μm thick) were rehydrated in graded ethanol. Endogenous peroxidase was blocked by incubating sections in PBS containing 1% H_2O_2 for 30 min at room temperature (RT). After several washes in PBS, the sections

were treated with the blocking buffer (1% normal goat serum in PBS; Sigma, St. Louis, MO, USA) for 30 min at room temperature. After several washes in PBS, sections were incubated in blocking buffer overnight at 4 °C with monoclonal anti-human CD31 (10G9, 1 : 150 dilution, sc-13537, Santa Cruz), anti-human CD34 (ICO115, 1 : 150 dilution, sc-7324, Santa Cruz), anti-human VEGFR2 (D-8, dilution 1 : 25, sc-393163, Santa Cruz), as well as rabbit polyclonal anti-Ki67 (AB9260, dilution 1 : 25, Millipore). After several rinses in PBS, sections were incubated with the secondary antibody goat anti-rabbit HRP-conjugate (dilution 1 : 20, G21234, Life technologies) or anti-mouse-HRP (dilution 1 : 100, A8924, Sigma) in blocking buffer for 1 h at RT. After several washes in PBS, the immunolabelling was visualized by incubation with 3-3′-diaminobenzidine- H_2O_2 medium for 10 min at RT. Sections were stained with the PAS methods. Finally, two sections for slide were counterstained with Hematoxylin and then, dehydrated, cleared, and mounted with Entellan. Negative controls were performed by omitting the primary antibodies.

Statistical analysis

A two-tailed Student's *t* test was performed assuming unequal variances to compare Panc1 cells and Panc1 CSCs and to determine whether the differences between two groups were statistically significant. ANOVA (post hoc Bonferroni) analysis was performed by GraphPad Prism 5 (GraphPad Software). *P*-values < 0.05, 0.01, or 0.001 were indicated as *, **, or ***, respectively, when compared to each control for each matrix and †, ††, or ††† compared to the same CM treatment on 100% Matrigel.

Acknowledgements

We thank Ivana Cataldo and Borislav Rusev for their support and suggestions in the histological analyses of the vascular network during the *in vivo* experiments. This work was supported by "Associazione Italiana per la Ricerca sul Cancro" (AIRC) grant #11348 to SJR. KZ was a fellow of the Marie Curie Initial Training Network IonTraC (FP7-PEOPLE-2011-ITN Grant Agreement No. 289648), ID is a fellow of the Fondazione Umberto Veronesi and EDP is a fellow of AIRC 5 per mille grant no. 12182. The SJR laboratory is part of the Italian network "Istituto Nazionale Biostrutture e Biosistemi" (INBB), the Centro di Eccellenza di Genomica in Campo Biomedico ed Agrario of the University of Bari and the project Bio-BoP of the Region Puglia. Action Co-founded by Cohesion and Development Fund 2007-2013 – APQ Research Puglia Region "Regional programme supporting smart specialization and social and environmental sustainability – FutureInResearch".

Conflict of interest

All authors declare that they have no conflict of interest.

Author contributions

SJR, MP, RAC, VC, GB, and KZ organized the project, designed the experiments and wrote the manuscript. MRG, SC, ID, EDP, and SF conducted the *in vitro* and *in vivo* experiments, performed the image analyses, and statistical evaluation. MM conducted the IHC analyses in the tumor sections.

References

1 Hong SM, Park JY, Hruban RH & Goggins M (2011) Molecular signatures of pancreatic cancer. *Arch Pathol Lab Med* **135**, 716–727.
2 Di Marco M, Grassi E, Durante S, Vecchiarelli S, Palloni A, Macchini M, Casadei R, Ricci C, Panzacchi R, Santini D *et al.* (2016) State of the art biological therapies in pancreatic cancer. *World J Gastrointest Oncol* **8**, 55–66.
3 Hidalgo M, Cascinu S, Kleeff J, Labianca R, Lohr JM, Neoptolemos J, Real FX, Van Laethem JL & Heinemann V (2015) Addressing the challenges of pancreatic cancer: future directions for improving outcomes. *Pancreatology* **15**, 8–18.
4 Schober M, Jesenofsky R, Faissner R, Weidenauer C, Hagmann W, Michl P, Heuchel RL, Haas SL & Lohr JM (2014) Desmoplasia and chemoresistance in pancreatic cancer. *Cancers (Basel)* **6**, 2137–2154.
5 Neesse A, Michl P, Frese KK, Feig C, Cook N, Jacobetz MA, Lolkema MP, Buchholz M, Olive KP, Gress TM *et al.* (2011) Stromal biology and therapy in pancreatic cancer. *Gut* **60**, 861–868.
6 ing H, Dey P, Yao W, Kimmelman AC, Draetta GF, Maitra A & DePinho RA (2016) Genetics and biology of pancreatic ductal adenocarcinoma. *Genes Dev* **30**, 355–385.
7 Dalla Pozza E, Forciniti S, Palmieri M & Dando I (2017) Secreted molecules inducing epithelial-to-mesenchymal transition in cancer development. *Semin Cell Dev Biol*. doi: S1084-9521(16)30486-4 [pii] https://doi.org/10.1016/j.semcdb.2017.06.027.

8 Whatcott CJ, Diep CH, Jiang P, Watanabe A, LoBello J, Sima C, Hostetter G, Shepard HM, Von Hoff DD & Han H (2015) Desmoplasia in primary tumors and metastatic lesions of pancreatic cancer. *Clin Cancer Res* **21**, 3561–3568.
9 Shields MA, Dangi-Garimella S, Redig AJ & Munshi HG (2012) Biochemical role of the collagen-rich tumour microenvironment in pancreatic cancer progression. *Biochem J* **441**, 541–552.
10 Koenig A, Mueller C, Hasel C, Adler G & Menke A (2006) Collagen type I induces disruption of E-cadherin-mediated cell-cell contacts and promotes proliferation of pancreatic carcinoma cells. *Cancer Res* **66**, 4662–4671.
11 Hamada S, Masamune A & Shimosegawa T (2013) Alteration of pancreatic cancer cell functions by tumor-stromal cell interaction. *Front Physiol* **4**, 318.
12 Marjanovic ND, Weinberg RA & Chaffer CL (2013) Cell plasticity and heterogeneity in cancer. *Clin Chem* **59**, 168–179.
13 Kure S, Matsuda Y, Hagio M, Ueda J, Naito Z & Ishiwata T (2012) Expression of cancer stem cell markers in pancreatic intraepithelial neoplasias and pancreatic ductal adenocarcinomas. *Int J Oncol* **41**, 1314–1324.
14 Dalla Pozza E, Dando I, Biondani G, Brandi J, Costanzo C, Zoratti E, Fassan M, Boschi F, Melisi D, Cecconi D *et al.* (2014) Pancreatic ductal adenocarcinoma cell lines display a plastic ability to bidirectionally convert into cancer stem cells. *Int J Oncol* **46**, 1099–1108.
15 Zhan HX, Xu JW, Wu D, Zhang TP & Hu SY (2015) Pancreatic cancer stem cells: new insight into a stubborn disease. *Cancer Lett* **357**, 429–437.
16 Li C, Wu JJ, Hynes M, Dosch J, Sarkar B, Welling TH, Pasca di Magliano M & Simeone DM (2011) c-Met is a marker of pancreatic cancer stem cells and therapeutic target. *Gastroenterology* **141**, 2218–2227. e2215.
17 Castellanos JA, Merchant NB & Nagathihalli NS (2013) Emerging targets in pancreatic cancer: epithelial-mesenchymal transition and cancer stem cells. *Onco Targets Ther* **6**, 1261–1267.
18 Rhim AD, Mirek ET, Aiello NM, Maitra A, Bailey JM, McAllister F, Reichert M, Beatty GL, Rustgi AK, Vonderheide RH *et al.* (2012) EMT and dissemination precede pancreatic tumor formation. *Cell* **148**, 349–361.
19 Lee CJ, Dosch J & Simeone DM (2008) Pancreatic cancer stem cells. *J Clin Oncol* **26**, 2806–2812.
20 Hanahan D & Coussens LM (2012) Accessories to the crime: functions of cells recruited to the tumor microenvironment. *Cancer Cell* **21**, 309–322.
21 DeClerck YA (2012) Desmoplasia: a response or a niche? *Cancer Discov* **2**, 772–774.
22 Minami Y (2015) Overview: cancer stem cell and tumor environment. *Oncology* **89** (Suppl 1), 22–24.
23 Pageau SC, Sazonova OV, Wong JY, Soto AM & Sonnenschein C (2011) The effect of stromal components on the modulation of the phenotype of human bronchial epithelial cells in 3D culture. *Biomaterials* **32**, 7169–7180.
24 Brizzi MF, Tarone G & Defilippi P (2012) Extracellular matrix, integrins, and growth factors as tailors of the stem cell niche. *Curr Opin Cell Biol* **24**, 645–651.
25 Zanoni M, Piccinini F, Arienti C, Zamagni A, Santi S, Polico R, Bevilacqua A & Tesei A (2016) 3D tumor spheroid models for *in vitro* therapeutic screening: a systematic approach to enhance the biological relevance of data obtained. *Sci Rep* **6**, 19103.
26 Xu X, Farach-Carson MC & Jia X (2014) Three-dimensional *in vitro* tumor models for cancer research and drug evaluation. *Biotechnol Adv* **32**, 1256–1268.
27 Zeeberg K, Cardone RA, Greco MR, Saccomano M, Nohr-Nielsen A, Alves F, Pedersen SF & Reshkin SJ (2016) Assessment of different 3D culture systems to study tumor phenotype and chemosensitivity in pancreatic ductal adenocarcinoma. *Int J Oncol* **49**, 243–252.
28 Vellinga TT, den Uil S, Rinkes IH, Marvin D, Ponsioen B, Alvarez-Varela A, Fatrai S, Scheele C, Zwijnenburg DA, Snippert H *et al.* (2010) Collagen-rich stroma in aggressive colon tumors induces mesenchymal gene expression and tumor cell invasion. *Oncogene* **35**, 5263–5271.
29 Deer EL, Gonzalez-Hernandez J, Coursen JD, Shea JE, Ngatia J, Scaife CL, Firpo MA & Mulvihill SJ (2010) Phenotype and genotype of pancreatic cancer cell lines. *Pancreas* **39**, 425–435.
30 Fan YL, Zheng M, Tang YL & Liang XH (2013) A new perspective of vasculogenic mimicry: EMT and cancer stem cells (Review). *Oncol Lett* **6**, 1174–1180.
31 Godugu C, Patel AR, Desai U, Andey T, Sams A & Singh M (2013) AlgiMatrix based 3D cell culture system as an in-vitro tumor model for anticancer studies. *PLoS ONE* **8**, e53708.
32 Cardone RA, Greco MR, Zeeberg K, Zaccagnino A, Saccomano M, Bellizzi A, Bruns P, Menga M, Pilarsky P, Schwab A *et al.* (2015) A novel NHE1-centered signaling cassette drives epidermal growth factor receptor–dependent pancreatic tumor metastasis and is a target for combination therapy. *Neoplasia* **17**, 155–166.
33 Hartel M, Di Mola FF, Gardini A, Zimmermann A, Di Sebastiano P, Guweidhi A, Innocenti P, Giese T, Giese N, Buchler MW *et al.* (2004) Desmoplastic reaction influences pancreatic cancer growth behavior. *World J Surg* **28**, 818–825.
34 Chu GC, Kimmelman AC, Hezel AF & DePinho RA (2007) Stromal biology of pancreatic cancer. *J Cell Biochem* **101**, 887–907.
35 Farmakovskaya M, Khromova N, Rybko V, Dugina V, Kopnin B & Kopnin P (2016) E-Cadherin repression increases amount of cancer stem cells in human A549

lung adenocarcinoma and stimulates tumor growth. *Cell Cycle* **15**, 1084–1092.
36 Zhang S, Guo H, Zhang D, Zhang W, Zhao X, Ren Z & Sun B (2006) Microcirculation patterns in different stages of melanoma growth. *Oncol Rep* **15**, 15–20.
37 Busco G, Cardone RA, Greco MR, Bellizzi A, Colella M, Antelmi E, Mancini MT, Dell'Aquila ME, Casavola V, Paradiso A *et al.* (2010) NHE1 promotes invadopodial ECM proteolysis through acidification of the peri-invadopodial space. *FASEB J* **24**, 3903–3915.
38 Wang LM, Silva MA, D'Costa Z, Bockelmann R, Soonawalla Z, Liu S, O'Neill E, Mukherjee S, McKenna WG, Muschel R *et al.* (2016) The prognostic role of desmoplastic stroma in pancreatic ductal adenocarcinoma. *Oncotarget* **7**, 4183–4194.
39 Jung J (2014) Human tumor xenograft models for preclinical assessment of anticancer drug development. *Toxicol Res* **30**, 1–5.
40 Shen Y, Quan J, Wang M, Li S, Yang J, Lv M, Chen Z, Zhang L & Zhao X (2017) Tumor vasculogenic mimicry formation as an unfavorable prognostic indicator in patients with breast cancer. *Oncotarget* **8**, 56408–56416.
41 Holmes K, Roberts OL, Thomas AM & Cross MJ (2007) Vascular endothelial growth factor receptor-2: structure, function, intracellular signalling and therapeutic inhibition. *Cell Signal* **19**, 2003–2012.
42 Qiao L, Liang N, Zhang J, Xie J, Liu F, Xu D, Yu X & Tian Y (2015) Advanced research on vasculogenic mimicry in cancer. *J Cell Mol Med* **19**, 315–326.
43 Simons M, Gordon E & Claesson-Welsh L (2016) Mechanisms and regulation of endothelial VEGF receptor signalling. *Nat Rev Mol Cell Biol* **17**, 611–625.
44 Williamson SC, Metcalf RL, Trapani F, Mohan S, Antonello J, Abbott B, Leong HS, Chester CP, Simms N, Polanski R *et al.* (2016) Vasculogenic mimicry in small cell lung cancer. *Nat Commun* **7**, 13322.
45 Shields MA, Dangi-Garimella S, Krantz SB, Bentrem DJ & Munshi HG (2011) Pancreatic cancer cells respond to type I collagen by inducing snail expression to promote membrane type 1 matrix metalloproteinase-dependent collagen invasion. *J Biol Chem* **286**, 10495–10504.
46 Paulis YW, Huijbers EJ, van der Schaft DW, Soetekouw PM, Pauwels P, Tjan-Heijnen VC & Griffioen AW (2015) CD44 enhances tumor aggressiveness by promoting tumor cell plasticity. *Oncotarget* **6**, 19634–19646.
47 Bailey JM, Alsina J, Rasheed ZA, McAllister FM, Fu YY, Plentz R, Zhang H, Pasricha PJ, Bardeesy N, Matsui W *et al.* (2014) DCLK1 marks a morphologically distinct subpopulation of cells with stem cell properties in preinvasive pancreatic cancer. *Gastroenterology* **146**, 245–256.
48 Elshamy WM & Duhe RJ (2013) Overview: cellular plasticity, cancer stem cells and metastasis. *Cancer Lett* **341**, 2–8.
49 Zhao Y, Bao Q, Renner A, Camaj P, Eichhorn M, Ischenko I, Angele M, Kleespies A, Jauch KW & Bruns C (2011) Cancer stem cells and angiogenesis. *Int J Dev Biol* **55**, 477–482.
50 Bonnet D & Dick JE (1997) Human acute myeloid leukemia is organized as a hierarchy that originates from a primitive hematopoietic cell. *Nat Med* **3**, 730–737.
51 Malanchi I, Peinado H, Kassen D, Hussenet T, Metzger D, Chambon P, Huber M, Hohl D, Cano A, Birchmeier W *et al.* (2008) Cutaneous cancer stem cell maintenance is dependent on beta-catenin signalling. *Nature* **452**, 650–653.
52 Lapouge G, Beck B, Nassar D, Dubois C, Dekoninck S & Blanpain C (2012) Skin squamous cell carcinoma propagating cells increase with tumour progression and invasiveness. *EMBO J* **31**, 4563–4575.
53 Mao XG, Xue XY, Wang L, Zhang X, Yan M, Tu YY, Lin W, Jiang XF, Ren HG, Zhang W *et al.* (2013) CDH5 is specifically activated in glioblastoma stemlike cells and contributes to vasculogenic mimicry induced by hypoxia. *Neuro Oncol* **15**, 865–879.
54 Rafiee P, Ogawa H, Heidemann J, Li MS, Aslam M, Lamirand TH, Fisher PJ, Graewin SJ, Dwinell MB, Johnson CP *et al.* (2003) Isolation and characterization of human esophageal microvascular endothelial cells: mechanisms of inflammatory activation. *Am J Physiol Gastrointest Liver Physiol* **285**, G1277–G1292.
55 Ricci-Vitiani L, Pallini R, Biffoni M, Todaro M, Invernici G, Cenci T, Maira G, Parati EA, Stassi G, Larocca LM *et al.* (2010) Tumour vascularization via endothelial differentiation of glioblastoma stem-like cells. *Nature* **468**, 824–828.
56 Dittmer J & Leyh B (2014) Paracrine effects of stem cells in wound healing and cancer progression (Review). *Int J Oncol* **44**, 1789–1798.
57 Zhang S, Fu Z, Wei J, Guo J, Liu M & Du K (2015) Peroxiredoxin 2 is involved in vasculogenic mimicry formation by targeting VEGFR2 activation in colorectal cancer. *Med Oncol* **32**, 414.
58 Narayanan V & Weekes CD (2016) Molecular therapeutics in pancreas cancer. *World J Gastrointest Oncol* **8**, 366–379.
59 Kim Y, Han D, Min H, Jin J & Yi EC (2014) Comparative proteomic profiling of pancreatic ductal adenocarcinoma cell lines. *Mol Cells* **37**, 888–898.